Author Manuscript

Author Manuscript

Author Manuscript

Author Manuscript

HHS Public Access

Author manuscript

Sci Immunol. Author manuscript; available in PMC 2024 January 27.

Published in final edited form as:

Sci Immunol. 2023 October 20; 8(88): eadg7597. doi:10.1126/sciimmunol.adg7597.

Integrin α3 promotes Th17 cell polarization and extravasation during autoimmune neuroinflammation.

Eunchong Park[1,2], **William E. Barclay**[1], **Alejandro Barrera**[2,3], **Tzu-Chieh Liao**[1,2], **Harmony R. Salzler**[1], **Timothy E. Reddy**[2,3], **Mari L. Shinohara**[1,4], **Maria Ciofani**[1,2,4,*]

[1]Department of Integrative Immunobiology, Duke University Medical Center, Durham, NC, USA

[2]Center for Advanced Genomic Technologies, Duke University, Durham, NC, USA

[3]Department of Biostatistics and Bioinformatics, Duke University Medical School, Durham, NC, USA

[4]Department of Molecular Genetics and Microbiology, Duke University Medical Center, Durham, NC, USA

Abstract

Multiple sclerosis (MS) is an autoimmune disease of the central nervous system (CNS) caused by CNS-infiltrating leukocytes, including Th17 cells that are critical mediators of disease pathogenesis. While targeting leukocyte trafficking is effective in treating autoimmunity, there are currently no therapeutic interventions that specifically block encephalitogenic Th17 cell migration. Here, we report integrin α3 as a Th17 cell-selective determinant of pathogenicity in experimental autoimmune encephalomyelitis. CNS-infiltrating Th17 cells express high integrin α3 and its deletion in $CD4^+$ T cells or *Il17a* fate-mapped cells attenuated disease severity. Mechanistically, integrin α3 enhanced the immunological synapse formation to promote the polarization and proliferation of Th17 cells. Moreover, the transmigration of Th17 cells into the CNS was dependent on integrin α3, and integrin α3-deficiency enhanced the retention of $CD4^+$ T cells in the perivascular space of the blood-brain barrier. Notably, integrin α3-dependent interactions continuously maintain Th17 cell identity and effector function. The requirement of integrin α3 in Th17 cell pathogenicity suggests integrin α3 as a therapeutic target for MS treatment.

One sentence summary

Integrin α3 promotes Th17 cell differentiation, proliferation and transmigration, driving pathogenicity during autoimmune neuroinflammation

*Correspondence: maria.ciofani@duke.edu.

Author contributions

E. P. designed, performed, and analyzed most experiments; W. E. B. designed, performed, and analyzed immunohistochemistry experiments; A. B. analyzed RNA-seq data; T. L. performed *C. rodentium* infection experiment; H. R. S. performed experiments; T. E. R. provided expertise of computational analysis; M. L. S. provided reagents and EAE model expertise; E. P. and M. C. wrote the manuscript; M. C. conceived the study, designed, supervised, and analyzed experiments.

Competing interests

The authors have no competing interests.

Author Manuscript Author Manuscript Author Manuscript Author Manuscript

Introduction

Multiple sclerosis (MS) is an autoimmune disease of the central nervous system (CNS). The infiltration of autoreactive $CD4^+$ T cells into the CNS is a critical step in disease pathogenesis, causing a neurodegenerative process characterized by the demyelination of neuronal axons (1). Experimental autoimmune encephalomyelitis (EAE), a murine model of MS, has elucidated the pivotal role of $CD4^+$ T cells in autoimmune neuroinflammation, as the adoptive transfer of myelin-reactive $CD4^+$ T cells is sufficient to induce EAE in naïve recipients (2, 3). Among $CD4^+$ helper T (Th) cell effector subsets, Th1 cells—defined by T-bet and IFNγ expression—were initially considered to be the main pathogenic cells in MS (4, 5), however, mice lacking IFNγ or IL-12 remain susceptible to EAE (6–8). Rather, the discovery that the Th17 cell-promoting cytokine IL-23 is required for autoimmune neuroinflammation identified Th17 cells as the key pathogenic Th subset in MS and EAE (8–11).

Th17 cells are a heterogenous subset characterized by the expression of IL-17A/F and RORγt. Th17 cells generated at steady-state promote homeostasis of mucosal barriers, whereas those elicited by IL-23 and IL-1β express IFNγ and GM-CSF and promote autoimmunity (12–16). Such inflammatory Th17 cells clear fungal and bacterial infections, but also contribute to the pathogenesis of MS and EAE (17–19). Indeed, elevated frequencies of Th17 cells in the blood and cerebrospinal fluid (CSF) of MS patients are correlated with disease activity (18–20). Moreover, human Th17 cells display greater migration potential and cytotoxic activity against neurons than Th1 cells; and Th17 cell-derived IL-17 promotes the disruption of the blood-brain barrier (BBB) and CNS inflammation (21). Therefore, understanding the basis of Th17 cell pathogenicity is crucial to the development of MS therapeutics.

One effective strategy in treating autoimmune disease is blocking lymphocyte infiltration into inflamed tissues. Natalizumab inhibits the migration of Th1 cells into the CNS of MS patients by targeting integrin α4 (22). However, its long-term use increases the risk of opportunistic viral infection in the brain leading to progressive multifocal leukoencephalopathy (23–25). Importantly, natalizumab is ineffective in inhibiting Th17 cell migration due to low levels of integrin α4 expression (26) and the availability of other adhesion mechanisms for CNS entry (27). Rather, natalizumab treatment can enhance Th17 cell pathogenicity and brain infiltration capacity (28). Therefore, elucidating the migratory mechanisms of Th17 cells can provide alternative strategies to inhibit encephalitogenic T cell infiltration into the CNS.

Various integrins, adhesion molecules, and chemokine receptors contribute to T cell migration during neuroinflammation, including LFA-1 (29), integrin α4β7 (30), MCAM (31), MAdCAM-1 (32), JAM-B (33), and CCR6 (34), although, most are not exclusively expressed by Th17 cells. While CCR6 is highly expressed by Th17 cells, encephalitogenic Th17 cells downregulate CCR6 expression (14, 35), and CCR6-deficient mice develop more severe—albeit delayed—EAE (36, 37). In addition, clinical trials targeting CCR1 or CCR2 in MS patients failed due to poor efficacy (38, 39). Recent studies reported roles for integrin

Author Manuscript Author Manuscript Author Manuscript Author Manuscript

αvβ3 and DICAM in Th17 cell pathogenicity during EAE (40, 41), however, they have yet to be evaluated for their clinical benefits.

Motivated to identify therapeutic targets regulating Th17 cell-specific migration, we discovered that integrin α3 is selectively expressed by Th17 cells during EAE. Integrins are heterodimeric transmembrane proteins that regulate cell adhesion and migration (42). VLA-3 (integrin α3β1) interacts with extracellular matrix (ECM) to mediate epithelial cell adhesion to basement membranes (43–46). Its ligands include ECM molecules such as collagens, fibronectins, and laminins (47). Laminins are heterotrimeric proteins comprised of α, β, and γ chains and enriched in the basal lamina (48). Among laminins, laminin α5 exhibits strong affinity for integrin α3, and integrin α3-laminin α5 interaction can initiate cell migration (49–51). A function for integrin α3 in cell migration has been described for various cell types (50, 52–56), however, its role in $CD4^+$ T cells has not been characterized.

Given this pro-migratory role of integrin α3 and the presence of laminin α5 in lymph nodes and vascular endothelial basement membrane including the BBB (57, 58), we hypothesized that integrin α3 is required for Th17 cell migration into the CNS during EAE pathogenesis. In this study, we demonstrate that integrin α3 promotes not only the CNS extravasation of Th17 cells but also the effective polarization and expansion of Th17 cells. These results indicate that integrin α3 is a critical determinant of Th17 cell pathogenicity in EAE and suggest that blockade of integrin α3 can be therapeutically advantageous for the treatment of MS and other Th17 cell-mediated autoimmune disorders.

Results

Integrin α3 is selectively expressed by Th17 cells

We previously reported that mice lacking JunB in T cells are resistant to EAE development, and JunB-deficient $CD4^+$ T cells fail to infiltrate into the CNS (59). This suggests that JunB regulatory targets can identify genes involved in encephalitogenic T cell migration. Indeed, pathway analysis of the differentially expressed genes (DEGs) in JunB-deficient Th17 cells revealed enrichment of migration-related pathways (fig. S1A). Among the 65 DEGs related to lymphocyte migration (Fig. 1A), *Itga3* (encoding integrin α3) stood out as it is induced in Th17 cells (60), and its role in T cells remains unknown.

To assess *Itga3* specificity, we compared its expression among *in vitro*-polarized mouse Th and Treg cell subsets. *Itga3* transcript levels were highest in Th17 cell subsets, with greater expression in pathogenic (p)Th17 versus conventional Th17 cells, and with over 40-fold higher expression in pTh17 cultures than naïve $CD4^+$ T cells or Th0, Th1, Th2, and Treg cultures (Fig. 1B). Accordingly, integrin α3 protein was exclusively detected in Th17 and pTh17 cells (Fig. 1, C and D, and fig. S1B). We also examined integrin α3 expression on human $CD4^+$ T cell subsets differentiated from peripheral blood mononuclear cell (PBMC)-derived naïve $CD4^+$ T cells under Th0, Th1, Treg, and Th17-polarizing conditions (fig. S1C). Similarly, uniformly high levels of integrin α3 expression were selective to human Th17 cell-promoting cultures (Fig. 1E) and maintained on PBMC-isolated memory Th17 cells, which express significantly higher levels of integrin α3 compared to memory Th1 and $CD45RO^+$ Treg cells (fig. S1D). Therefore, integrin α3 is exclusively induced in mouse

Author Manuscript Author Manuscript Author Manuscript Author Manuscript

and human Th17 cell specialization. This degree of Th17 cell-specificity is unique among integrins; integrins α6 and αv are required for lymphocyte migration in EAE (61) and skin inflammation (62), however, they are broadly expressed across Th and Treg cell subsets (fig. S1E). Furthermore, the mRNA expression level of *Itga4*—the target of natalizumab—is low in Th17 cells compared to Th1 cells consistent with previous reports (26, 63) (fig. S1E).

To understand the basis of Th17 cell-specific *Itga3* expression, we evaluated *Itga3* regulation by Th17 cell-specifying transcription factors (TFs) BATF, IRF4, STAT3, and lineage-defining RORγt (60). Relative to wild-type cells, deletion of any of these specifying TFs significantly reduced *Itga3* transcript levels in Th17 cell cultures (Fig. 1B and fig. S1F). In addition, ChIP-seq analysis revealed these TFs also occupy putative enhancers upstream of *Itga3* that are marked by binding of the histone acetyltransferase p300 (Fig. 1G). Collectively, these findings indicate that, in addition to JunB, *Itga3* expression is directly activated by BATF, IRF4, STAT3, and RORγt, such that exclusive expression of *Itga3* in Th17 cells results from high order combinatorial regulation by Th17 cell-specifying TFs.

Integrin α3 is expressed by Th17 cells during EAE.

We next assessed integrin α3 expression by peripheral $CD4^+$ T cells in *wild-type (WT)* mice; cells from $Itga3^{fl/fl}$ CD4-Cre (KO^{CD4}) mice that lack *Itga3* expression in T cells served as negative staining controls. Unlike *in vitro*-differentiated pTh17 cells, steady-state Th17 and Th1 cells in the inguinal lymph nodes (iLNs) or spleen of naïve mice expressed very low or undetectable levels of integrin α3 (fig. S2A).

Since Th17 cells are critical for EAE pathogenesis (11), we investigated whether Th17 cells elicited during EAE express integrin α3. At EAE onset, Th17 cells in iLNs and spleen, and Treg cells in spleen expressed low levels of integrin α3 (fig. S2B). Notably, integrin α3 expression was further increased by IL-17A-producing Th17 cells in the spinal cord at both the onset and peak of EAE, including encephalitogenic Th17.1 cells co-expressing IL-17A and IFNγ (Fig. 2, A and B, and fig. S2C). Integrin α3 was also expressed by $Foxp3^+$ Treg cells in the CNS, but at a lower level than Th17 cells (Fig. 2, A and B, and fig. S2C). Interestingly, $IFN\gamma^+$ $CD4^+$ Th1-like cells in the spinal cord at disease peak expressed similar levels of integrin α3 as Th17 cells (Fig. 2B); this is in contrast to the undetectable levels of integrin α3 for *in vitro*-differentiated Th1 cells (Fig. 1, C and D). As most Th1 cells derive from Th17 cells during EAE (14), we assessed whether integrin $\alpha3^+$ Th1 cells in the CNS are ex-Th17 cells that retain integrin α3 expression. For this, we induced EAE in $Il17a^{Cre/+}$ $Rosa26^{lsl\text{-}Zsgreen}$ (WT^{Il17a} $R26^{ZG}$) fate-mapping mice in which cells with a history of *Il17a* expression are permanently marked by ZsGreen (ZG) expression from the *Rosa26* locus. Comparison of ZG^+ and ZG^- $IFN\gamma^+$ $CD4^+$ T cells in the spinal cord at EAE peak confirmed that integrin α3 expression was detectable on ZG^+ ex-Th17 cells but not ZG^- *bona fide* Th1 cells (Fig. 2C). Thus, high-level integrin α3 expression is exclusive to pathogenic Th17 and $IFN\gamma^+$ ex-Th17 cells in the context of EAE.

To explore whether integrin α3 is modulated during MS, we interrogated transcriptomic data comparing $CD4^+$ T cells isolated from the CSF versus the blood of MS patients (64). Migration-related significantly DEGs included *ITGA3*, *ITGA4*, *ITGA6*, and the heterodimerization partner of integrin α3, *ITGB1* (Fig. 2D). Notably, expression of *ITGA3*

Author Manuscript Author Manuscript Author Manuscript Author Manuscript

is elevated in CSF CD4$^+$ T cells to a similar extent as natalizumab therapy target *ITGA4* (1.6- and1.7-fold, respectively). In contrast, expression of *ITGA6*, another laminin-binding integrin, is decreased in CSF CD4$^+$ T cells. The increased level of VLA-3 on human CSF CD4$^+$ T cells suggests integrin α3 contributes to effector functions of CD4$^+$ T cells in MS pathogenesis.

Itga3 expression is induced by the IL-6-STAT3 pathway.

The selective induction of *Itga3* by Th17/pTh17-promoting conditions suggested a role for IL-6 in *Itga3* activation. Indeed, culturing naïve CD4$^+$ T cells in the presence of IL-6 significantly induced integrin α3 expression in a dose-dependent manner (Fig. 3A, r=0.90). Conversely, *Stat3*-deficient CD4$^+$ T cells failed to upregulate *Itga3* transcripts in response to IL-6, which remain at a level similar to wild-type naïve CD4$^+$ T cells (Fig. 3B), thus, corroborating that the IL-6-Stat3 signal pathway is required for *Itga3* expression in CD4$^+$ T cells.

We further tested the influence of pTh17-driving IL-1β and IL-23 on integrin α3 expression, since pTh17 cultures express higher levels of integrin α3 compared to Th17 cells polarized by IL-6 and TGF-β. IL-1β or IL-23 did not induce integrin α3 expression when added individually or in combination, however, they synergized with IL-6 to enhance integrin α3 levels (Fig. 3C). Conversely, integrin α3 expression in pTh17 cultures was significantly downregulated by TGF-β in a dose-dependent manner (Fig. 3D, r=−0.9). Therefore, the IL-6-STAT3 pathway activates integrin α3 expression, which is antagonized by TGF-β signals, thus promoting a selective pattern of expression by Th17 cells.

T cell development is unaltered in the absence of *Itga3*

To further study integrin α3, we conditionally deleted *Itga3* in T cells by breeding *Itga3*$^{fl/fl}$ mice to the CD4-Cre deleter strain and used *Itga3*$^{fl/fl}$ or CD4-Cre mice as *wild-type* (*WT*) controls. *Itga3* deletion in *Itga3*$^{fl/fl}$ CD4-Cre (*KO*^{CD4}) mice did not affect total thymocytes numbers, or positive selection as marked by TCRβ and CD69 expression (fig. S3A). The cellularity and the frequency of CD4$^+$ TCRβ$^+$ cells and CD8$^+$ TCRβ$^+$ cells were unaltered in the iLNs and spleen of *KO*^{CD4} mice (fig. S3B), indicating that T cell distribution into secondary lymphoid organs is integrin α3-independent. CD4$^+$ T cell development was also unaffected by *Itga3* deletion, as the frequencies and numbers of naïve CD44^{lo}CD62L^{hi} CD4$^+$ T cells, Treg, Th1, and Th17 cells were comparable between *WT* and *KO*^{CD4} mice at steady-state (fig. S3, B and C). There were no significant differences in the numbers and frequencies of CD4$^+$ T cell populations in the small intestine lamina propria of *KO*^{CD4} mice, including homeostatic Th17, Th1, or Foxp3$^+$ Treg cells (fig. S3D). Moreover, the comparable abundance of segmented filamentous bacteria (SFB), which is regulated by homeostatic Th17 cells (65), demonstrates unaltered effector function of intestinal homeostatic Th17 cells in *KO*^{CD4} mice (fig. S3E). With T cell development intact, the *KO*^{CD4} model allowed us to investigate the role of *Itga3* in inflammatory contexts.

Deletion of *Itga3* attenuates EAE and CNS infiltration

To assess the role of *Itga3* in CD4$^+$ T cells in neuroinflammatory disease, EAE was induced in *WT* and *KO*^{CD4} mice by immunization with MOG$_{35–55}$ peptides. While *WT* mice

Author Manuscript Author Manuscript Author Manuscript Author Manuscript

developed severe clinical symptoms of EAE, KO^{CD4} mice exhibited significantly delayed disease onset and reduced disease severity (Fig. 4A). Notably, although the frequencies of Th1, Th17, and Treg cells were comparable between *WT* and KO^{CD4} mice in the spinal cord at peak disease, there was a 2.5-fold decrease in the number of $CD4^+$ T cells in KO^{CD4} mice (Fig. 4, B and C). Consistently, the numbers of spinal cord Th17 and Th1 cells were reduced in KO^{CD4} mice compared to *WT* mice by 2.8-fold and 2.0-fold, respectively (Fig. 4C). These differences were already evident at EAE symptom onset—with a greater than 3-fold decrease in the number of Th17, Th1, Treg, and total $CD4^+$ T cells in KO^{CD4} spinal cords (fig. S4A)—likely contributing to delayed disease onset in KO^{CD4} mice.

We next evaluated whether *Itga3* deficiency affects $CD4^+$ T cell migration into the CNS. CNS-infiltrating lymphocytes must penetrate the BBB, which is formed by vascular endothelial cells, basement membranes enriched with laminins, pericytes, and astrocyte end-feet covering the CNS parenchyma (66). Since the parenchymal basement membrane is less permissive than the endothelial basement membrane, lymphocytes transiently collect in the perivascular space between membranes before traversing into the spinal cord parenchyma, forming a structure called an inflammatory perivascular cuff (58, 67) (Fig. 4D). Defects in lymphocyte migration from the perivascular space to the parenchyma delay disease onset (67). At the peak of EAE, spinal cord sections of *WT* mice were characterized by greatly enlarged perivascular spaces and significantly higher numbers of infiltrating $CD4^+$ T cells versus KO^{CD4} mice (Fig. 4D), indicating defective $CD4^+$ T cell transmigration to the perivascular space in KO^{CD4} mice. Consistent with flow cytometric analysis, the number of $CD4^+$ T cells per field image of KO^{CD4} spinal cord sections was 2-fold less than that of *WT* sections (Fig. 4D). Additionally, the ratio of $CD4^+$ T cell numbers in the parenchyma relative to that in the perivascular space was 4-fold less in KO^{CD4} mice, indicative of enhanced perivascular retention of $CD4^+$ T cells in KO^{CD4} versus *WT* spinal cords (Fig. 4D). This reveals a defect in CNS infiltration for $CD4^+$ T cells lacking integrin α3, which contributes to the delayed disease onset and milder EAE symptoms of KO^{CD4} mice.

We induced EAE in WT^{Il17a} $R26^{ZG}$ and KO^{Il17a} $R26^{ZG}$ mice to assess the requirement for *Itga3* when *Itga3 is* selectively deleted in Th17 cells after specification via $Il17a^{Cre}$. The significantly attenuated EAE severity observed in KO^{CD4} mice was recapitulated in KO^{Il17a} $R26^{ZG}$ mice (Fig. 4E), suggesting that integrin α3 is required for Th17 cell neuropathogenicity. However, *Itga3* loss in other IL-17A-expressing cells, particularly γδ T cells and innate lymphoid cells that have roles in EAE (68, 69), may contribute to ameliorated disease in KO^{Il17a} $R26^{ZG}$ mice. To directly test the requirement of *Itga3* in Th17 cells, we employed passive EAE. In this model, $CD4^+$ T cells expressing the transgenic 2D2 TCR recognizing $MOG_{35–55}$ peptide are differentiated into pTh17 or Th1 cells *in vitro*, and adoptively transferred into $Tcra^{-/-}$ mice to induce disease (70). Mice receiving KO^{CD4} 2D2 pTh17 cells developed significantly milder EAE with delayed onset compared to mice receiving *WT* 2D2 pTh17 cells (Fig. 4F), corroborating that the loss of *Itga3* in Th17 cells is sufficient to attenuate EAE. Conversely, transfer of 2D2 Th1 cells induced severe EAE irrespective of *Itga3* genotype (Fig. 4G), indicating that Th17 cells are selectively integrin α3-dependent for encephalitogenic function.

Author Manuscript Author Manuscript Author Manuscript Author Manuscript

To understand the cellular mechanisms by which *Itga3* deficiency in T cells reduced CD4$^+$ T cell numbers in the spinal cord, we analyzed draining iLNs at day 10 of EAE, prior to symptom onset when expanded effector CD4$^+$ T cells begin to migrate into the CNS. At EAE pre-onset, the numbers of Th17 and Treg cells in iLNs were already modestly, but significantly reduced in KO^{CD4} versus *WT* mice, with Th1 cell numbers also trending lower in KO^{CD4} mice (fig. S4B). Notably, at this early time point post-EAE induction, *WT* Th17 cell frequencies and counts formed bimodal distributions: intermediate and high. Interestingly, KO^{CD4} Th17 proportions and numbers were elevated above those of naïve KO^{CD4} mice, and nearly to the intermediate level of *WT* mice, suggesting Th17 polarization is delayed or ineffective without integrin α3 (fig. S4B).

Integrin α3 promotes Th17 cell polarization and proliferation.

The reduced number of Th17 cells in iLNs of KO^{CD4} mice at EAE pre-onset suggests integrin α3 promotes Th17 cell differentiation or proliferation during inflammation. To test this, we adoptively transferred proliferation dye-loaded and CD45-congenically-marked *WT* (CD45.1$^+$) and KO^{CD4} (CD45.1$^-$) naïve 2D2 CD4$^+$ T cells at a 1:1 ratio into EAE-induced $Tcra^{-/-}$ mice, thus polarizing *WT* and KO^{CD4} cells in the same environment *in vivo* (Fig. 5A). At 24 h post-transfer, the KO^{CD4}:*WT* ratio of naïve CD4$^+$ T cells in the inoculum was maintained in the iLNs of recipient mice, indicating that migration of KO^{CD4} naïve CD4$^+$ T cells into iLNs is not *Itga3*-dependent (Fig. 5B). This is consistent with naïve CD4$^+$ T cells lacking integrin α3 expression (Fig. 1, C and D) and the unaltered distribution of naïve CD4$^+$ T cells in iLNs of steady-state KO^{CD4} mice (fig. S3B). Moreover, loss of CD62L and upregulation of CD44 expression by *WT* and KO^{CD4} CD4$^+$ T cells was comparable at 24 h post immunization, demonstrating their similarly productive initial interaction with antigen presenting cells (APCs) (Fig. 5C).

Despite unaffected initial activation, by 60 h post-immunization, KO^{CD4} 2D2 CD4$^+$ T cells generated reduced frequencies of RORγt$^+$ cells with significantly lower RORγt expression levels compared to *WT* cells (Fig. 5D). Indeed, similar modest differences in RORγt expression have functional outcomes in type 3 cells (71). To mitigate potential confounding effects of proliferation, we compared non-proliferating G0 cells and the frequency of RORγt$^+$ cells was also decreased for KO^{CD4} 2D2 CD4$^+$ T cells, revealing compromised Th17 cell polarization with *Itga3* deficiency (Fig. 5D). Conversely, the frequency of T-bet$^+$ cells was slightly higher for KO^{CD4} versus *WT* 2D2 CD4$^+$ T cells (21.1% versus 19.6%). *Itga3* deficiency also resulted in defects in Th17 cell proliferation; when comparing the proliferation index of RORγt$^+$ cells, KO^{CD4} 2D2 CD4$^+$ T cells proliferated less than *WT* counterparts (Fig. 5D). However, the proliferation index of total CD4$^+$ T cells, RORγt$^-$ CD4$^+$ T cells, and T-bet$^+$ CD4$^+$ T cells was unaltered between *WT* and KO^{CD4} cells, highlighting the selective importance of integrin α3 in supporting Th17 cell proliferation (Fig. 5D).

By day 7 of EAE, the relative contribution of KO^{CD4} 2D2 CD4$^+$ T cells was significantly decreased compared to day 2.5 or 1 (Fig. 5B), likely resulting from the cumulative effect of defective proliferation of KO^{CD4} cells. The unchanged ratio of KO^{CD4} 2D2 CD4$^+$ T cells in naïve mice at day 7 post transfer confirms that the differential expansion between KO^{CD4}

Author Manuscript Author Manuscript Author Manuscript Author Manuscript

and *WT* CD4$^+$ T cells is antigen-dependent (Fig. 5B). The early defects in proliferation and RORγt expression resulted in significantly fewer IL-17A-producing CD4$^+$ T cells among *KO^{CD4}* compared to *WT* 2D2 CD4$^+$ T cells by day 7 of EAE (Fig. 5E). Consistent with the increased T-bet$^+$ population after 60 h, the frequency of IFNγ-producing CD4$^+$ T cells was higher in *KO^{CD4}* versus *WT* cells (Fig. 5E).

Unlike differentiation during EAE, *in vitro* polarization of *WT* and *KO^{CD4}* naïve CD4$^+$ T cells into Th17 cells or other Th and Treg subsets did not exhibit differences in polarization or proliferation when TCR stimulation was provided by plate-bound anti-CD3ε and anti-CD28 antibodies (fig. S5, A and B). Therefore, integrin α3 deficiency does not affect intrinsic signaling pathways driving T cell polarization or proliferation. However, Th17 and pTh17 cell differentiation induced by mitomycin C-treated splenocytes selectively showed reduced polarization and proliferation of *KO^{CD4}* CD4$^+$ T cells (fig. S5C), whereas *KO^{CD4}* Th1 and Treg cells were unaffected. Therefore, splenocytes provide signals—potentially via adhesion molecules that interact with integrin α3—that promote integrin α3-dependent differentiation and expansion of Th17 subsets.

Integrin α3β1-mediated interaction promotes TCR stimulation.

We next investigated whether integrin α3 influences the Th17 cell-APC interaction. We evaluated iLN cells isolated from EAE-induced mice for the expression of adhesion molecules that interact with integrin α3 by incubating cells with His-tagged recombinant integrin α3β1 (rVLA-3). Flow cytometric analysis with anti-His antibody revealed binding of rVLA-3 to MHCII-expressing APCs, including dendritic cells (DCs) and a small fraction of B cells, but not to T cells (Fig. 6A). Notably, rVLA-3 bound to a large proportion of CD11b$^+$ DCs, a population of classical DCs specialized in inducing Th17 cells (72, 73). Consistent with the expression of integrin α3 ligands on DCs, rVLA-3 also bound to *in vitro*-differentiated bone marrow-derived DCs (BMDCs) (Fig. 6B).

Since integrins such as LFA-1 and VLA-4 strengthen immunological synapse (IS) formation (74–77), we evaluated whether integrin α3 enhances Th17 cell activation by facilitating T cell-APC interaction. For this, we co-cultured 2D2 pTh17 cells with BMDCs pulsed with $MOG_{35–55}$ peptide. Although *WT* and *KO^{CD4}* 2D2 pTh17 cells showed a similar level of conjugation with BMDCs (Fig. 6C), the MFI of CD3ε at the IS was significantly reduced for *KO^{CD4}* compared to *WT* 2D2 pTh17 cells (Fig. 6D), indicating weaker IS formation by *Itga3*-deficient pTh17 cells. This difference affected the phosphorylation of ERK, one of downstream signaling targets of the TCR, as ERK1/2 phosphorylation was modestly, but consistently decreased for *KO^{CD4}* versus *WT* 2D2 pTh17 cells (Fig. 6E). Therefore, adhesion molecules expressed by APCs bind to VLA-3 on Th17 cells and enable stronger IS formation and TCR signaling, leading to increased Th17 cell polarization and proliferation.

Integrin α3 maintains the Th17 cell program during EAE.

To investigate the role of integrin α3 in differentiated Th17 cells, we employed fate-mapping *Il17a^{Cre} R26^{ZG}* mice, allowing us to track Th17 or ex-Th17 cells marked by ZG, while selectively deleting *Itga3* from ZG$^+$ *KO^{Il17a} R26^{ZG}* CD4$^+$ T cells upon *Il17a* expression. To assess cells in the same environment, we adoptively transferred a 1:1 mixture of naïve 2D2

Author Manuscript Author Manuscript Author Manuscript Author Manuscript

CD4$^+$ T cells from *WT^{Il17a} R26^{ZG}* 2D2 (CD45.1$^+$) and *KO^{Il17a} R26^{ZG}* 2D2 (CD45.1$^-$) mice into *Tcra*$^{-/-}$ recipients, and induced EAE the following day (Fig. 7A). We analyzed recipient mice at EAE clinical score of 1.5. Notably, the frequency of ZG$^+$ cells—representing Th17 or ex-Th17 cells—was significantly smaller for *KO^{Il17a}* versus *WT^{Il17a}* 2D2 CD4$^+$ T cells in every tissue examined, including iLN, spleen, blood, and spinal cord (Fig. 7B). As *Itga3* is deleted after Th17 cell specification, the reduced frequency of ZG$^+$ cells in the *KO^{Il17a}* CD4$^+$ T cell compartment demonstrates that integrin α3 continuously promotes Th17 cell expansion or survival. Moreover, *Itga3*-deficient *Il17a* fate-mapped ZG$^+$ CD4$^+$ T cells also lost IL-17A expression in the periphery, with significant IL-17A loss in the iLN, blood, and spinal cord (Fig. 7C). Instead, peripheral *Itga3*-deficient ZG$^+$ CD4$^+$ T cells acquired higher proportions and levels of IFNγ expression, as either IL-17A$^+$ IFNγ$^+$ Th17.1 cells or IL-17A$^-$ IFNγ$^+$ ex-Th17 cells (Fig. 7C). Therefore, Th17 cells continuously require integrin α3 to expand and maintain IL-17A expression.

To uncover how integrin α3 affects Th17 cell stability, we performed RNA-seq comparing *WT^{Il17a}* and *KO^{Il17a}* 2D2 ZG$^+$ CD4$^+$ T cells sorted from the iLNs of EAE-induced *Tcra*$^{-/-}$ recipients 7 days post-immunization (Fig. 7, A and D). The majority of DEGs were downregulated upon *Itga3* deletion (Fig. 7D), including a striking abundance of Th17 effector and signature genes (e.g., *Rorc*, *Rora*, *Irf4*, *Ahr*, *Il17re*, *Il23r*, *Il9r*, *Il1r1*, and *Il22*) (Fig. 7, D and E), consistent with a broad depletion of Th17 features in the absence of *Itga3*. Conversely, Th1-related genes (e.g., *Tbx21* and *Il12rb2*) were upregulated with *Itga3* deletion (Fig. 7, D and E). Consistently, evaluation of the dysregulated transcriptome in *KO^{Il17a}* 2D2 ZG$^+$ CD4$^+$ T cells using gene set enrichment analysis (GSEA) revealed that the most downregulated genes were significantly enriched for Th17 signature genes, whereas the most upregulated genes were enriched for Th1 signature genes (Fig. 7F). These global alterations in effector program reveal that integrin α3 supports Th17 cell identity during EAE induction.

Pathway analysis of the top DEGs revealed a downregulation of the neuroinflammation signaling pathway, highlighting that integrin α3 drives CNS autoimmunity (Fig. 7G). Together, pathway analysis and GSEA support the role of integrin α3 in Th17 cell differentiation as pathways related to Th17 cell polarization (e.g., IL-6/JAK/STAT3, HIF1α, IL-23, TGF-β, and GM-CSF signaling) were significantly downregulated in *KO^{Il17a}* ZG$^+$ CD4$^+$ T cells (Fig. 7, F and G). T-cell activation and TCR signaling pathways—including MAPK activation—were downregulated in *KO^{Il17a}* ZG$^+$ CD4$^+$ T cells (Fig. 7, F and G), supporting that integrin α3 enhances TCR signal intensity or duration to promote proliferation and maintain Th17 cell identity.

Significantly enriched pathways related to cell transmigration and GPCR signaling were also downregulated in *KO^{Il17a}* ZG$^+$ CD4$^+$ T cells (Fig. 7, F and G). GPCR signals activate chemokine receptors and downstream cell migration. In particular, the expression of numerous chemokines (e.g., *Ccl6*, *Ccl8*, and *Ccl24*), chemokine receptors (e.g., *Ccr4*, *Ccr6*, and *Cxcr4*), and integrins (e.g., *Itgav* and *Itgb3*) was depleted (Fig. 7E), indicating that integrin α3 engagement impacts broader chemotaxis and migration programs in Th17 cells, and that *Itga3*-deletion may result in multiple defects in the migration of encephalitogenic

Author Manuscript Author Manuscript Author Manuscript Author Manuscript

Th17 cells. Of note, integrin αvβ3 (product of *Itgav* and *Itgb3*) (40) and CCR6 (34) contribute to Th17 cell CNS infiltration during EAE.

Lastly, cell death-related pathways were suppressed in KO^{Il17a} ZG^+ $CD4^+$ T cells (Fig. 7G), encompassing significant reductions in the expression of pro-apoptotic genes including apoptosome factor *Apaf1*, transcriptional repressor *Rbl2*, TNF receptors (*Tnfrsf1b* and *Tnfrsf25*), and *Bcl2l11* (). This suggests that the decreased relative frequency of KO^{Il17a} ZG^+ $CD4^+$ T cells in EAE-induced $Tcra^{-/-}$ recipients is attributable to reduced expansion and not enhanced cell death. Collectively, these findings support a model in which *Itga3* loss in Th17 cells alters the global transcriptome regulating Th17 cell polarization, T-cell activation, and migration.

Integrin α3 promotes Th17 cell infiltration into the CNS.

Integrins regulate cell migration via adhesion to the extracellular matrix or blood vessel endothelium, and initiation of intracellular signals that reorganize cytoskeletal structure (78). Pathway analyses highlight that integrin α3 promotes the expression of migration-related genes in encephalitogenic Th17 cells (Fig. 7, F and G). To specifically address whether integrin α3 is required for the CNS transmigration of Th17 cells during EAE, we used the naïve 2D2 $CD4^+$ T cell WT^{Il17a}:KO^{Il17a} competitive transfer model described in Fig. 7A. When EAE-induced $Tcra^{-/-}$ recipient mice reached a clinical score of 1.5, we analyzed the relative contribution of KO^{Il17a} cells within the ZG^+ $CD4^+$ T cell compartment across different organs. We observed a striking and significant decrease in the relative proportion of KO^{Il17a} ZG^+ 2D2 $CD4^+$ T cells in the spinal cord compared to the blood and spleen (Fig. 8A). This decrease of KO^{Il17a} $CD4^+$ T cells in the CNS supports the hypothesis that *Itga3*-deficient Th17 cells do not efficiently migrate into the spinal cord and instead, accumulate in the periphery.

To bypass the role of integrin α3 during *in vivo* T cell priming and Th17 cell induction, we employed a competitive passive EAE model. We transferred *in vitro*-polarized 2D2 pTh17 cells—with *WT* 2D2 ($CD45.1^+$) and KO^{CD4} 2D2 ($CD45.1^-$) cells at a 1:1 ratio—into $Tcra^{-/-}$ mice (Fig. 8B) and assessed the relative proportion of KO^{CD4} cells in the periphery and CNS at day 14. The relative percentage of KO^{CD4} cells in the spinal cord was significantly decreased compared to that in the spleen or blood, comprising only 24% of $CD4^+$ T cells (Fig. 8B). Importantly, this reduction does not reflect a defect in pTh17 cell survival as KO^{CD4} cells did not undergo increased apoptotic cell death compared to *WT* cells in the spinal cord (fig. S7). Rather, *WT* cells displayed greater apoptotic markers in the spleen and spinal cord (fig. S7), consistent with the reduced cell death signatures in KO^{Il17a} ZG^+ $CD4^+$ T cells (Fig. 7G). The relative accumulation of KO^{CD4} cells in the spleen and blood highlights the essential role of integrin α3 in permitting CNS infiltration of pTh17 cells, independent of its function in Th17 cell priming and development *in vivo*.

We next investigated whether the role of integrin α3 is specific to the CNS or if it is generally required for Th17 cell immunity and migration into inflamed tissues. For this, we orally infected *WT* and KO^{CD4} mice with *Citrobacter rodentium,* which elicits inflammatory Th17 cells required for bacterial clearance in the colon (79, 80). In comparing *WT* and KO^{CD4} mice at 1, 2, and 3 weeks post infection, both genotypes displayed similar *C.*

Author Manuscript Author Manuscript Author Manuscript Author Manuscript

rodentium bacterial loads and clearance in the colon and feces (fig. S6A). Notably, integrin α3 expression by colonic Th17, Th1, and Treg cells 3 weeks post infection was low relative to maximal levels observed during EAE (fig. S6B and Fig. 2B). $CD4^+$ T cells significantly expanded in the colon during *C. rodentium* infection (fig. S6C), with no difference in the frequencies and numbers of Th1, Th17, Treg, or total $CD4^+$ T cells between *WT* and KO^{CD4} mice (fig. S6C and S6D). Therefore, in contrast to its role in EAE pathogenesis, integrin α3 is not essential for the expansion, migration, or effector function of Th17 cells for protective immunity during colonic inflammation.

Inside-out activation of integrins mediates lymphocyte arrest on the vascular endothelium (81). The detection of VLA-3 ligands on DCs (Fig. 6, A and B), prompted us to investigate whether vascular endothelial cells also express VLA-3-interacting adhesion molecules. We confirmed that b.End3 cells, a mouse brain vascular endothelial cell line, express adhesion molecules that bind to rVLA-3 (Fig. 8, C and D), suggesting that integrin α3 directly facilitates Th17 cell arrest on vascular endothelium.

Following lymphocyte arrest, ECM ligand-induced outside-in integrin signaling can promote lymphocyte migration via cytoskeletal remodeling (82). The perivascular space is bordered by basement membranes rich in laminins α4, α5, α1, and α2 (Fig. 4C). Thus, integrin α3-expressing Th17 cells can respond to laminin α5 as they penetrate the BBB. We therefore investigated whether laminin α5 can stimulate integrin α3 on Th17 cells to promote cell motility using a transwell migration assay. Pre-coating transwells with laminin α5 significantly enhanced *WT* Th17 and pTh17 cell migration (Fig. 8E). This was largely integrin α3-dependent as *Itga3* deficiency significantly reduced the migration of KO^{CD4} compared to *WT* Th17 and pTh17 cells. Similarly, laminin α5 also promoted human Th17 cell migration, and blockade using inhibitory anti-integrin α3 antibody (P1B5) significantly reduced migration across the transwell (Fig. 8F). Therefore, laminin α5-mediated outside-in activation of integrin α3 promotes Th17 cell migration. Moreover, Th17 and pTh17 cells cultured with plate-bound laminin α5 underwent morphological changes such as the elongation of cell bodies, suggesting that integrin α3 stimulation induces active cytoskeletal rearrangements (fig. S8). These findings collectively support a model whereby integrin α3-ligand interactions promote Th17 cell infiltration into the spinal cord during EAE pathogenesis.

Discussion

The CNS is an immune-privileged site where the BBB restricts leukocyte infiltration. Nevertheless, encephalitogenic leukocytes penetrate the barrier and exacerbate CNS inflammation in MS and EAE. Integrins and adhesion molecules facilitate $CD4^+$ T cell CNS infiltration; however, factors that selectively mediate the migration of encephalitogenic Th17 cells are less characterized (29–31, 40, 83). Here, we define integrin α3 as a nonredundant and selective regulator of Th17 cell pathology in the context of neuroinflammation. We demonstrate that integrin α3 promotes Th17 cell polarization, proliferation, and infiltration into the CNS during EAE, and, as such propose integrin α3 as a potential therapeutic target for MS treatment.

Author Manuscript Author Manuscript Author Manuscript Author Manuscript

Despite well-defined roles for integrin α3 in organogenesis and tumorigenesis (43–45, 54, 55), its function in immune cells—in lymphocytes, in particular—remains largely unexplored. Among $CD4^+$ T cells, we found integrin α3 expression selectively induced during mouse and human Th17 cell differentiation *in vitro*, and on pTh17 cells in the context of EAE *in vivo*. This specific expression can be attributed to the direct coregulation of *Itga3* by Th17 cell specification factors, including JunB, BATF, IRF4, STAT3, and RORγt (59, 60, 84–87) and upstream Th17-inducing signals. Indeed, we show TCR signals (upstream of BATF and IRF4) and the IL-6 pathway (upstream of JunB and STAT3 activity) are necessary for the activation of *Itga3* expression. Conversely, TGF-β antagonizes *Itga3* expression. Mechanistically, TGF-β-induced signals, such as via Smad3, can interfere with the transcriptional activities of *Itga3* regulators STAT3 (88) and RORγt (89). While TGF-β is indispensable for encephalitogenic Th17 cell induction and EAE pathogenesis (90, 91), nonlimiting levels of TGF-β favor the differentiation of non-pathogenic Th17 cells (12). Thus, the TGF-β axis may fine-tune integrin a3 expression maximizing levels on pTh17 cells.

Integrin α3 is required for Th17 cell pathogenicity during EAE via several mechanisms, including promoting effective Th17 cell polarization and proliferation. Similar to JunB (59), integrin α3 is selectively required for pathogenic Th17 cell induction, but not for homeostatic Th17 cell differentiation. In this context, integrin α3 is continuously required to maintain IL-17A expression in Th17 cells elicited in EAE; rather, *Itga3*-deficient Th17 cells express IFNγ. This effector shift is supported by attenuated RORγt expression, enhanced T-bet proportions, and weaker TCR signaling in *Itga3*-deficiency. Indeed, TCR signaling strength impacts $CD4^+$ T cell effector differentiation (92, 93). Nevertheless, this shift is not simply enhanced conversion of Th17 cells into pathogenic Th1-like effectors typical of EAE as *Itga3*-deficiency downregulates pathogenesis-associated gene signatures for neuroinflammation, TCR signaling, and migration. Taken together, integrin α3 promotes the effective induction and maintenance of the pathogenic Th17 cell program.

We demonstrate that integrin α3 facilitates effective Th17 cell differentiation and proliferation via cell-cell interaction, and iLN DCs and BMDCs express adhesion molecules that engage with integrin α3 on Th17 cells. Indeed, integrins interact with various non-integrin cell adhesion molecules expressed on immune cells and endothelial cells, such as ICAMs, VCAM-1, MadCAM-1, selectins, and JAMs (94). In particular, the trans-heterophilic interactions between integrins (e.g., LFA-1 and VLA-4) and adhesion molecules (e.g., ICAM-1, VCAM-1, and JAM-A) play a crucial role in the formation of the IS and consequent T cell polarization (74–77). Similarly, we found that integrin α3 enhances IS formation and p-ERK1/2 signaling in pTh17 cells upon contact with BMDCs. Therefore, VLA-3-mediated cell-cell interaction favors Th17 cell polarization and proliferation by strengthening the IS (92, 93).

Integrin α3β1 signals may also enhance Th17 cell polarization and proliferation via crosstalk with TCR signals. Integrin α3 signals via PI3K and ERK (50, 95), whereas integrin β chains can activate Syk, ZAP-70, ERK, Akt, and NF-κB pathways (96–98), all of which are critical components of TCR signaling. Notably, integrin α3-stimulating ligands, such as laminins, collagens, and fibronectins, are available in the LN environment (57, 99).

Author Manuscript Author Manuscript Author Manuscript Author Manuscript

It is tempting to speculate that signaling downstream of integrin α3 engagement enhances TCR signals to promote Th17 cell polarization and proliferation. Additionally, via its effect on Th17 cell motility, integrin α3 activation may increase the contact frequency between Th17 cells and APCs to enhance Th17 cell induction. In support of such synergy, loss of integrin α3 downregulates a TCR signaling signature in Th17 cells.

Integrin α3 enables Th17 cell pathogenicity by promoting CNS transmigration. In a competitive EAE setting, *Itga3*-deficient 2D2 Th17 cells are disadvantaged relative to *WT* cells in spinal cord entry. *Itga3*-deficient $CD4^+$ T cells also show greater retention in the blood vessel perivascular space and reduced infiltration into the spinal cord parenchyma. Importantly, the basement membranes of BBB vessels are rich in integrin α3 ligands, including laminin α5 (58), providing a mechanistic rationale for integrin α3-promoted Th17 cell CNS infiltration. Indeed, laminin α5 enhances Th17 cell motility *in vitro*, and the laminin-rich structure of the BBB may similarly enhance Th17 cell infiltration. Interestingly, laminin α5 can play a protective role in EAE by promoting BBB integrity, and consequently limiting CNS infiltration of lymphocytes (58, 100). While we show that integrin α3 can be exploited for effective penetration of the BBB, this likely relies on an array of ligands in addition to laminin α5. Furthermore, integrin α3 could promote Th17 cell arrest on the BBB endothelium given that b.End3 brain vascular endothelial cells express adhesion molecules that bind rVLA-3. Thus, further investigation is needed to identify these integrin α3-interaction targets. Lastly, integrin α3 deficiency in Th17 cells results in the reduced expression of other integrins (e.g., *Itgav* and *Itgb3*) and chemokine receptors (e.g., *Ccr4*, *Ccr6*, and *Cxcr4*), some with known roles in EAE pathogenesis (101). Thus, integrin α3 engagement licenses a broader migration program in Th17 cells, the global downregulation of which likely contributes to CNS infiltration defects.

The requirement for integrin α3 in inflammatory Th17 cell effector function is context-dependent. Integrin α3 is expressed by Th17 cells induced in both the chronic autoimmune context of EAE and protective immunity to *C. rodentium*. However, in contrast to EAE, Th17 cell migration to the colon elicited by *C. rodentium* is integrin α3-independent. Several distinctions between EAE and *C. rodentium* infection may account for this difference. First, the $CD4^+$ T cell response could be more robust in infection versus EAE as foreign antigens generally trigger stronger TCR stimulation than autoantigens (102), thereby potentially overcoming the dependence on auxiliary interactions. Second, the intestine is more accessible than the CNS, which is tightly secured by the BBB. Lastly, the intestine has different barrier structures (e.g., MAdCAM-1, selectins, and collagens) from the BBB (103), thus lymphocytes require distinct machineries for migration into the intestine (e.g., integrins α4β7, α4β1, αEβ7, and CCR9) (104–106), which may compensate for the loss of integrin α3. Lastly, colonic $CD4^+$ T cells express low levels of integrin α3. This may be attributable to the high-TGF-β-environment of the colon (107), which can suppress integrin α3 expression, resulting in a less significant role for integrin α3 in colon compared to CNS inflammation.

Our findings support the therapeutic potential of targeting integrin α3 to block Th17 cell CNS infiltration in MS. Considering that pathogenic Th1 cells in EAE are mainly derived from Th17 cell conversion (14) and that human Th17 cells promote BBB disruption

Author Manuscript Author Manuscript Author Manuscript Author Manuscript

and possess greater migration potential than Th1 cells (21), the development of therapies specifically targeting Th17 cell migration via integrin α3 blockade may improve clinical outcomes in MS, either alone or in combination with natalizumab treatment. Indeed, using a passive EAE model, we demonstrate integrin α3 selectively promotes Th17 cell CNS migration; whereas Th17 cells require integrin α3 to elicit severe EAE, Th1 cells are completely independent of integrin α3 for pathogenesis. As a proof-of-principle in support of integrin α3 as a therapeutic target, we show that an inhibitory integrin α3 antibody diminishes human Th17 cell transmigration *in vitro*. However, lack of a commercial inhibitory antibody for mouse integrin α3 has precluded assessment of the therapeutic benefit of integrin α3 blockade in EAE, which is an important future goal. In this regard, as integrin α3 is expressed by various myeloid cells (52, 53, 108), it will be critical to evaluate possible off-target effects of integrin α3 blockade in pre-clinical studies. Taken together, we have identified integrin α3 as a selective and critical determinant of pathogenic Th17 cell differentiation, expansion, and CNS infiltration during EAE. As such, integrin α3 represents a potential target for therapeutic intervention in MS.

Materials and methods

Study design

We aimed to determine the role of integrin α3 in Th17 cell pathogenicity during autoimmune neuroinflammation. We used the EAE disease model, in conjunction with transgenic and conditional knock-out mice to validate the requirements of integrin α3 in Th17 cell polarization and migration. Data were analyzed using flow cytometry, microscopy, RT-qPCR, Western blot, and RNA-seq methods. No data points or outliers were excluded. For *C. rodentium* infection, mice that produced colonies from steady-state fecal material on MacConkey Agar were not used in experiments evaluating bacterial clearance. The numbers of independent experiments, pooling of multiple experiments, and statistical methods are indicated in the figure legends. Required sample size for hypothesis testing in mouse experiments was determined by Mead's equation. Mice were assigned to experimental groups by block randomization taking into consideration sex, age range, and cage for cohousing WT and KO genotypes. Samples were unblinded. Reagents used in this study are provided in table S1. The study follows ARRIVE 2.0 Guidelines for pre-clinical animal study reporting.

Human T cell samples

Peripheral blood from deidentified healthy adult donors were obtained with informed consent by the Duke Substrate Services Core with approval from the Duke University Health System Institutional Review Board.

Mice

Itga3$^{fl/fl}$ (#008818), *Il17a*$^{Cre/+}$ (#016879), *CD4-Cre* (#022071), *Rosa26*$^{lsl\text{-}Zsgreen/WT}$ (#007906), 2D2 TCR transgenic (#006912), CD45.1^{+} congenic (#002014), *Stat3*$^{fl/fl}$ (#016923), and *Tcra* KO (#002116) mice were obtained from the Jackson Laboratory. Mice were bred and maintained in specific-pathogen-free facilities at Duke University and used in accordance with the Duke Institutional Animal Care and Use Committee guidelines.

Author Manuscript Author Manuscript Author Manuscript Author Manuscript

Experimental mice were used between 8 and 14 weeks of age with no preference for sex, except for adoptive transfer of $CD4^+$ T cells, where donors and recipients were sex-matched. Co-housed experimental mice and littermate controls were used.

BMDC culture and antigen pulse

Mouse BM cells were differentiated into DCs. Briefly, BM cells ($1X10^5$/ml) were cultured in RPMI 1640 supplemented with 10% FBS, HEPES (10 mM), sodium pyruvate (1 mM), glutamine (2 mM), penicillin (10 U/ml), streptomycin (10 μg/ml), gentamicin (50 μg/ml), and β-mercaptoethanol (55 μM) (complete RPMI) plus GM-CSF (20 ng/ml). At day 7, loosely adherent cells were harvested. To pulse BMDCs with $MOG_{35–55}$ peptide, BMDCs ($5X10^6$/ml) were incubated in the presence of $MOG_{35–55}$ peptide (100 μg/ml) and LPS (200 ng/ml) for 24 h.

pTh17 cell-BMDC co-culture

$3X10^4$ *in vitro*-cultured 2D2 pTh17 cells were co-cultured with $3X10^4$ $MOG_{35–55}$ peptide-pulsed BMDCs at 37°C for 5 min for phospho-ERK1/2 analysis or 30 min for immunofluorescence imaging. For immunofluorescence, cells were fixed with PFA (4%) for 30 min at room temperature, stained with Alexa Fluor 488-anti-CD3ε and Alexa Fluor 647-anti-MHCII, imaged by confocal microscopy, and analyzed using ImageJ software. Cell conjugation percentage was calculated by dividing the number of T cells interacting with BMDCs by the number of total T cells. The IS formation was analyzed by dividing CD3ε MFI at the synapse by CD3ε MFI at the non-synapse.

VLA-3 binding assay

iLN cells from day 7 EAE-induced mice, BMDCs, or b.End3 cells were surface-stained with antibodies for 15 min at 4°C: MHCII, CD3ε, CD19, CD11c, and CD11b for iLN cells; CD11c for BMDCs; ICAM-1 for b.End3 cells. Cells were washed with staining buffer, incubated with 6X His-tagged rVLA-3 (R&D Systems, #9374-A3–050) in staining buffer at room temperature for 20 min, washed with staining buffer, and then stained with an APC-anti-His tag antibody for 10 min at room temperature. rVLA-3 binding was assessed using flow cytometry or fluorescent live cell imaging.

Active EAE

10–14-week-old mice were injected subcutaneously on day 0 with $MOG_{35–55}$ peptide (200 μg, United Biosystems) emulsified in CFA supplemented with heat-killed *Mycobacterium tuberculosis* (2 mg/ml, VGD, Inc./Voigt Global). Mice were injected intraperitoneally with pertussis toxin (200 ng, List Biologicals) on days 0 and 2. Mice were assessed daily for symptoms and scored as follows: 0, no symptoms; 0.5, limp tail tip; 1.0, limp tail; 1.5, weakened hind limb movement; 2.0, partial paralysis of one hind limb; 2.5, partial paralysis of both hind limbs; 3.0, severe paralysis of both hind limbs with some movement of hind feet but not hind legs; 3.5, complete hind limb paralysis; 4.0, complete hind and partial front paralysis; 4.5, complete hind and front paralysis or death. Mice that reached score of 4.5 were deemed moribund and euthanized.

Author Manuscript Author Manuscript Author Manuscript Author Manuscript

Passive EAE

2D2 pTh17 cells or Th1 cells were adoptively transferred into *Tcra*$^{-/-}$ mice. Naïve 2D2 CD4^{+} T cells from 2D2 *Itga3*$^{fl/fl}$ *CD4-Cre* or 2D2 *Itga3*$^{fl/fl}$ mice were cultured *in vitro* in pTh17- or Th1-polarizing conditions. After 5 days, cells were washed with PBS three times and resuspended in PBS. 2X10^{6} cells were retro-orbitally injected into *Tcra*$^{-/-}$ mice. Some mice developed atypical EAE (109), and were scored as follows: 0, no symptoms; 1.0, mild ataxia and/or poor hind limb coordination; 1.5, weakened hind limb movement; 2.0, partial paralysis of one hind limb; 2.5, partial paralysis of both hind limbs; 3.0, inability to walk on a straight line (severe ataxia); 3.5, laying on side or complete hind limb paralysis; 4.0, rolling continuously unless supported; 4.5, moribund or death.

Transmigration assays

Transwell filters (5 μm, Costar) were coated with rhlaminin-511 (BioLamina), rhlaminin-521 (Thermo Fisher Scientific), or BSA in HBSS containing calcium and magnesium (HBSS+CaMg) (0.2 μg/cm^{2}) at 37°C for 2 h, and washed with HBSS+CaMg. 72-h-*in vitro*-polarized mouse pTh17, Th17, or 6-d-*in vitro*-polarized human Th17 cells in RPMI 1640 media supplemented with HEPES (10 mM), sodium pyruvate (1 mM), penicillin (10 U/ml), streptomycin (10 μg/ml), gentamicin (50 μg/ml), and β-mercaptoethanol (55 μM) (incomplete RPMI) were added to the transwell filters. Transmigration was induced with complete RPMI in the bottom chamber. To limit the contribution of CCR6, we used FBS as a general chemoattractant instead of CCL20. After 6 h at 37°C, the transmigrated cells were counted and expressed as a percentage of total cells added to the upper chamber. To neutralize human integrin α3, human Th17 cells were incubated in the presence of anti-integrin α3 antibody (Sigma-Aldrich, P1B5, 20 ng/ml) for 15 min at 37°C before addition to the transwell filters.

RNA-seq

2D2 naïve CD4^{+} T cells from *WT*^{Il17a} *R26*^{ZG} 2D2 (CD45.1^{+}) and *KO*^{Il17a} *R26*^{ZG} 2D2 (CD45.1^{-}) mice were transferred into *Tcra*$^{-/-}$ mice at a 1:1 ratio. EAE was induced on the following day. 7 days post immunization, iLNs from 10 recipients were pooled into one replicate. Three total replicates were prepared per genotype, and ZG^{+} CD45.1^{+} CD4^{+} T cells (*WT*) or ZG^{+} CD45.1^{-} CD4^{+} T cells (*KO*) were FACS-sorted. RNA was purified using the RNeasy Plus Micro Kit (Qiagen). The Duke Sequencing and Genomic Technologies Shared Resource facility preprepared libraries using SMARTer v3/v4 Ultra Low Input RNA-seq Kit (Takara Biosciences). Libraries were sequenced on the Illumina NextSeq 500 using 50-bp single-end mode at a depth of 160–170 million reads per sample.

RNA-seq differential expression analysis

RNA-seq samples were validated using FastQC v0.11.2 (Babraham Institute). The removal of adapters and bases from raw reads were performed with average quality score (Q; Phred33) of <20 using a 4-bp sliding window (SlidingWindow:4:20) with Trimmomatic v0.32 (110). STAR v2.4.1a (111) was used to align trimmed reads to the primary assembly of the GRCm38 mouse genome, and alignments containing noncanonical splice junctions were removed (--outFilterIntronMotifs RemoveNoncanonical).

Author Manuscript Author Manuscript Author Manuscript Author Manuscript

Aligned reads were assigned to genes in the GENCODE vM13 comprehensive gene annotation (112) using featureCounts (v1.4.6-p4) with default settings (113). Differential expression analysis was performed (DESeq2, v1.22.0) (114) on R (v3.5.1). Genes with low or no expression were removed from raw counts. DESeq function was used to normalize filtered counts by computing estimated size factors and dispersions for Negative Binomial distributed data. Significant DEGs were found using the nbinomWaldTest which tests the coefficients in the fitted Negative Binomial GLM using the previously calculated size factors and dispersion estimates. Genes having a Benjamini–Hochberg FDR <0.05 were considered significant. Log_2(fold change) values were shrunk toward zero using the shrinkage estimator from the apeglm R package (115). For transcript abundance, the rsem-calculate-expression function in the RSEM v1.2.21 package was used to compute transcripts per million (TPM) values (116).

Further RNA seq analysis is described in supplementary materials and methods.

Statistical analysis

Data were analyzed using GraphPad Prism. Two-tailed unpaired or paired Student's *t*-test were used to compare differences between groups with normal distribution. Mann-Whitney *U* test was used to compare differences between groups that are not normally distributed. One-way or two-way ANOVA tests were used for multiple comparisons between groups. To compare EAE clinical severity, the area under the curve (AUC) of EAE clinical scores was calculated for each mouse using the trapezoidal rule. For correlation analysis, Pearson's correlation test was used to calculate correlation coefficients (r) and p-values (p). $p < 0.05$ was considered statistically significant. *, $p < 0.05$; **, $p < 0.01$; ***, $p < 0.001$; ****, $p < 0.0001$; ns, not significant.

Supplementary Material

Refer to Web version on PubMed Central for supplementary material.

Acknowledgments

We thank Minsoo Kim (University of Rochester Medical Center) for advice on analyzing perivascular space and flow cytometric detection of integrin α3. We acknowledge the expert assistance of Nancy Martin and Lynn Martinek with FACS sorting.

Funding

This work was funded by NIH grants R01-GM115474 and R01-AI156186 to M. Ciofani, and grants R01-NS120417 (NIH) and RG-4536B2/1 (NMSS) to M.L. Shinohara. The analyses performed by A. Barrera was supported by NIH grant UM1-HG009428 to M. Ciofani and T.E. Reddy. E. Park was supported by The Kwanjeong Educational Foundation Scholarship.

Data and materials availability

All data needed to evaluate the conclusions in the paper are present in the paper or the Supplementary Materials. RNA-seq data that support the findings of this study have been deposited in the Gene Expression Omnibus. Accession code, GSE214418.

Author Manuscript Author Manuscript Author Manuscript Author Manuscript

References

1. Fletcher JM, Lalor SJ, Sweeney CM, Tubridy N, Mills KH, T cells in multiple sclerosis and experimental autoimmune encephalomyelitis. Clin Exp Immunol 162, 1–11 (2010). [PubMed: 20682002]
2. Fallis RJ, Raine CS, McFarlin DE, Chronic relapsing experimental allergic encephalomyelitis in SJL mice following the adoptive transfer of an epitope-specific T cell line. J Neuroimmunol 22, 93–105 (1989). [PubMed: 2466872]
3. Paterson PY, Transfer of allergic encephalomyelitis in rats by means of lymph node cells. J Exp Med 111, 119–136 (1960). [PubMed: 14430853]
4. Ando DG, Clayton J, Kono D, Urban JL, Sercarz EE, Encephalitogenic T cells in the B10.PL model of experimental allergic encephalomyelitis (EAE) are of the Th-1 lymphokine subtype. Cell Immunol 124, 132–143 (1989). [PubMed: 2478300]
5. Panitch HS, Hirsch RL, Haley AS, Johnson KP, Exacerbations of multiple sclerosis in patients treated with gamma interferon. Lancet 1, 893–895 (1987). [PubMed: 2882294]
6. Ferber IA, Brocke S, Taylor-Edwards C, Ridgway W, Dinisco C, Steinman L, Dalton D, Fathman CG, Mice with a disrupted IFN-gamma gene are susceptible to the induction of experimental autoimmune encephalomyelitis (EAE). J Immunol 156, 5–7 (1996). [PubMed: 8598493]
7. Becher B, Durell BG, Noelle RJ, Experimental autoimmune encephalitis and inflammation in the absence of interleukin-12. J Clin Invest 110, 493–497 (2002). [PubMed: 12189243]
8. Cua DJ, Sherlock J, Chen Y, Murphy CA, Joyce B, Seymour B, Lucian L, To W, Kwan S, Churakova T, Zurawski S, Wiekowski M, Lira SA, Gorman D, Kastelein RA, Sedgwick JD, Interleukin-23 rather than interleukin-12 is the critical cytokine for autoimmune inflammation of the brain. Nature 421, 744–748 (2003). [PubMed: 12610626]
9. Harrington LE, Hatton RD, Mangan PR, Turner H, Murphy TL, Murphy KM, Weaver CT, Interleukin 17-producing CD4+ effector T cells develop via a lineage distinct from the T helper type 1 and 2 lineages. Nat Immunol 6, 1123–1132 (2005). [PubMed: 16200070]
10. Park H, Li Z, Yang XO, Chang SH, Nurieva R, Wang YH, Wang Y, Hood L, Zhu Z, Tian Q, Dong C, A distinct lineage of CD4 T cells regulates tissue inflammation by producing interleukin 17. Nat Immunol 6, 1133–1141 (2005). [PubMed: 16200068]
11. Langrish CL, Chen Y, Blumenschein WM, Mattson J, Basham B, Sedgwick JD, McClanahan T, Kastelein RA, Cua DJ, IL-23 drives a pathogenic T cell population that induces autoimmune inflammation. J Exp Med 201, 233–240 (2005). [PubMed: 15657292]
12. McGeachy MJ, Bak-Jensen KS, Chen Y, Tato CM, Blumenschein W, McClanahan T, Cua DJ, TGF-beta and IL-6 drive the production of IL-17 and IL-10 by T cells and restrain T(H)-17 cell-mediated pathology. Nat Immunol 8, 1390–1397 (2007). [PubMed: 17994024]
13. McGeachy MJ, Chen Y, Tato CM, Laurence A, Joyce-Shaikh B, Blumenschein WM, McClanahan TK, O'Shea JJ, Cua DJ, The interleukin 23 receptor is essential for the terminal differentiation of interleukin 17-producing effector T helper cells in vivo. Nat Immunol 10, 314–324 (2009). [PubMed: 19182808]
14. Hirota K, Duarte JH, Veldhoen M, Hornsby E, Li Y, Cua DJ, Ahlfors H, Wilhelm C, Tolaini M, Menzel U, Garefalaki A, Potocnik AJ, Stockinger B, Fate mapping of IL-17-producing T cells in inflammatory responses. Nat Immunol 12, 255–263 (2011). [PubMed: 21278737]
15. Harbour SN, Maynard CL, Zindl CL, Schoeb TR, Weaver CT, Th17 cells give rise to Th1 cells that are required for the pathogenesis of colitis. Proc Natl Acad Sci U S A 112, 7061–7066 (2015). [PubMed: 26038559]
16. El-Behi M, Ciric B, Dai H, Yan Y, Cullimore M, Safavi F, Zhang GX, Dittel BN, Rostami A, The encephalitogenicity of T(H)17 cells is dependent on IL-1- and IL-23-induced production of the cytokine GM-CSF. Nat Immunol 12, 568–575 (2011). [PubMed: 21516111]
17. Bedoya SK, Lam B, Lau K, Larkin J 3rd, Th17 cells in immunity and autoimmunity. Clin Dev Immunol 2013, 986789 (2013). [PubMed: 24454481]
18. Tzartos JS, Friese MA, Craner MJ, Palace J, Newcombe J, Esiri MM, Fugger L, Interleukin-17 production in central nervous system-infiltrating T cells and glial cells is associated with active disease in multiple sclerosis. Am J Pathol 172, 146–155 (2008). [PubMed: 18156204]

Author Manuscript Author Manuscript Author Manuscript Author Manuscript

19. Matusevicius D, Kivisakk P, He B, Kostulas N, Ozenci V, Fredrikson S, Link H, Interleukin-17 mRNA expression in blood and CSF mononuclear cells is augmented in multiple sclerosis. Mult Scler 5, 101–104 (1999). [PubMed: 10335518]
20. Brucklacher-Waldert V, Stuerner K, Kolster M, Wolthausen J, Tolosa E, Phenotypical and functional characterization of T helper 17 cells in multiple sclerosis. Brain 132, 3329–3341 (2009). [PubMed: 19933767]
21. Kebir H, Kreymborg K, Ifergan I, Dodelet-Devillers A, Cayrol R, Bernard M, Giuliani F, Arbour N, Becher B, Prat A, Human TH17 lymphocytes promote blood-brain barrier disruption and central nervous system inflammation. Nat Med 13, 1173–1175 (2007). [PubMed: 17828272]
22. Steinman L, The discovery of natalizumab, a potent therapeutic for multiple sclerosis. J Cell Biol 199, 413–416 (2012). [PubMed: 23109666]
23. Hellwig K, Gold R, Progressive multifocal leukoencephalopathy and natalizumab. J Neurol 258, 1920–1928 (2011). [PubMed: 21647730]
24. Aly L, Yousef S, Schippling S, Jelcic I, Breiden P, Matschke J, Schulz R, Bofill-Mas S, Jones L, Demina V, Linnebank M, Ogg G, Girones R, Weber T, Sospedra M, Martin R, Central role of JC virus-specific CD4+ lymphocytes in progressive multi-focal leucoencephalopathy-immune reconstitution inflammatory syndrome. Brain 134, 2687–2702 (2011). [PubMed: 21908874]
25. Bloomgren G, Richman S, Hotermans C, Subramanyam M, Goelz S, Natarajan A, Lee S, Plavina T, Scanlon JV, Sandrock A, Bozic C, Risk of natalizumab-associated progressive multifocal leukoencephalopathy. N Engl J Med 366, 1870–1880 (2012). [PubMed: 22591293]
26. Rothhammer V, Heink S, Petermann F, Srivastava R, Claussen MC, Hemmer B, Korn T, Th17 lymphocytes traffic to the central nervous system independently of alpha4 integrin expression during EAE. J Exp Med 208, 2465–2476 (2011). [PubMed: 22025301]
27. Schneider-Hohendorf T, Rossaint J, Mohan H, Boning D, Breuer J, Kuhlmann T, Gross CC, Flanagan K, Sorokin L, Vestweber D, Zarbock A, Schwab N, Wiendl H, VLA-4 blockade promotes differential routes into human CNS involving PSGL-1 rolling of T cells and MCAM-adhesion of TH17 cells. J Exp Med 211, 1833–1846 (2014). [PubMed: 25135296]
28. Janoschka C, Lindner M, Koppers N, Starost L, Liebmann M, Eschborn M, Schneider-Hohendorf T, Windener F, Schafflick D, Fleck AK, Koch K, Deffner M, Schwarze AS, Schulte-Mecklenbeck A, Metz I, Meuth SG, Gross CC, Meyer Zu Horste G, Schwab N, Kuhlmann T, Wiendl H, Stoll M, Klotz L, Enhanced pathogenicity of Th17 cells due to natalizumab treatment: Implications for MS disease rebound. Proc Natl Acad Sci U S A 120, e2209944120 (2023).
29. Dusi S, Angiari S, Pietronigro EC, Lopez N, Angelini G, Zenaro E, Della Bianca V, Tosadori G, Paris F, Amoruso A, Carlucci T, Constantin G, Rossi B, LFA-1 Controls Th1 and Th17 Motility Behavior in the Inflamed Central Nervous System. Front Immunol 10, 2436 (2019). [PubMed: 31681316]
30. Duc D, Vigne S, Bernier-Latmani J, Yersin Y, Ruiz F, Gaia N, Leo S, Lazarevic V, Schrenzel J, Petrova TV, Pot C, Disrupting Myelin-Specific Th17 Cell Gut Homing Confers Protection in an Adoptive Transfer Experimental Autoimmune Encephalomyelitis. Cell Rep 29, 378–390 e374 (2019). [PubMed: 31597098]
31. Breuer J, Korpos E, Hannocks MJ, Schneider-Hohendorf T, Song J, Zondler L, Herich S, Flanagan K, Korn T, Zarbock A, Kuhlmann T, Sorokin L, Wiendl H, Schwab N, Blockade of MCAM/CD146 impedes CNS infiltration of T cells over the choroid plexus. J Neuroinflammation 15, 236 (2018). [PubMed: 30134924]
32. Kuhbandner K, Hammer A, Haase S, Terbrack E, Hoffmann A, Schippers A, Wagner N, Hussain RZ, Miller-Little WA, Koh AY, Stoolman JS, Segal BM, Linker RA, Stuve O, MAdCAM-1-Mediated Intestinal Lymphocyte Homing Is Critical for the Development of Active Experimental Autoimmune Encephalomyelitis. Front Immunol 10, 903 (2019). [PubMed: 31114574]
33. Tietz S, Perinat T, Greene G, Enzmann G, Deutsch U, Adams R, Imhof B, Aurrand-Lions M, Engelhardt B, Lack of junctional adhesion molecule (JAM)-B ameliorates experimental autoimmune encephalomyelitis. Brain Behav Immun 73, 3–20 (2018). [PubMed: 29920328]
34. Reboldi A, Coisne C, Baumjohann D, Benvenuto F, Bottinelli D, Lira S, Uccelli A, Lanzavecchia A, Engelhardt B, Sallusto F, C-C chemokine receptor 6-regulated entry of TH-17 cells into the CNS through the choroid plexus is required for the initiation of EAE. Nat Immunol 10, 514–523 (2009). [PubMed: 19305396]

Author Manuscript Author Manuscript Author Manuscript Author Manuscript

35. Kara EE, McKenzie DR, Bastow CR, Gregor CE, Fenix KA, Ogunniyi AD, Paton JC, Mack M, Pombal DR, Seillet C, Dubois B, Liston A, MacDonald KPA, Belz GT, Smyth MJ, Hill GR, Comerford I, McColl SR, CCR2 defines in vivo development and homing of IL-23-driven GM-CSF-producing Th17 cells. Nat Commun 6, 8644 (2015). [PubMed: 26511769]
36. Elhofy A, Depaolo RW, Lira SA, Lukacs NW, Karpus WJ, Mice deficient for CCR6 fail to control chronic experimental autoimmune encephalomyelitis. J Neuroimmunol 213, 91–99 (2009). [PubMed: 19535153]
37. Villares R, Cadenas V, Lozano M, Almonacid L, Zaballos A, Martinez AC, Varona R, CCR6 regulates EAE pathogenesis by controlling regulatory CD4+ T-cell recruitment to target tissues. Eur J Immunol 39, 1671–1681 (2009). [PubMed: 19499521]
38. Horuk R, Chemokine receptor antagonists: overcoming developmental hurdles. Nat Rev Drug Discov 8, 23–33 (2009). [PubMed: 19079127]
39. Pease J, Horuk R, Chemokine receptor antagonists. J Med Chem 55, 9363–9392 (2012). [PubMed: 22931505]
40. Du F, Garg AV, Kosar K, Majumder S, Kugler DG, Mir GH, Maggio M, Henkel M, Lacy-Hulbert A, McGeachy MJ, Inflammatory Th17 Cells Express Integrin alphavbeta3 for Pathogenic Function. Cell Rep 16, 1339–1351 (2016). [PubMed: 27452457]
41. Charabati M, Grasmuck C, Ghannam S, Bourbonniere L, Fournier AP, Lecuyer MA, Tastet O, Kebir H, Rebillard RM, Hoornaert C, Gowing E, Larouche S, Fortin O, Pittet C, Filali-Mouhim A, Lahav B, Moumdjian R, Bouthillier A, Girard M, Duquette P, Cayrol R, Peelen E, Quintana FJ, Antel JP, Flugel A, Larochelle C, Arbour N, Zandee S, Prat A, DICAM promotes TH17 lymphocyte trafficking across the blood-brain barrier during autoimmune neuroinflammation. Sci Transl Med 14, eabj0473 (2022).
42. Yonekawa K, Harlan JM, Targeting leukocyte integrins in human diseases. J Leukoc Biol 77, 129–140 (2005). [PubMed: 15548573]
43. Kreidberg JA, Donovan MJ, Goldstein SL, Rennke H, Shepherd K, Jones RC, Jaenisch R, Alpha 3 beta 1 integrin has a crucial role in kidney and lung organogenesis. Development 122, 3537–3547 (1996). [PubMed: 8951069]
44. Has C, Sparta G, Kiritsi D, Weibel L, Moeller A, Vega-Warner V, Waters A, He Y, Anikster Y, Esser P, Straub BK, Hausser I, Bockenhauer D, Dekel B, Hildebrandt F, Bruckner-Tuderman L, Laube GF, Integrin alpha3 mutations with kidney, lung, and skin disease. N Engl J Med 366, 1508–1514 (2012). [PubMed: 22512483]
45. DiPersio CM, Hodivala-Dilke KM, Jaenisch R, Kreidberg JA, Hynes RO, alpha3beta1 Integrin is required for normal development of the epidermal basement membrane. J Cell Biol 137, 729–742 (1997). [PubMed: 9151677]
46. Anton ES, Kreidberg JA, Rakic P, Distinct functions of alpha3 and alpha(v) integrin receptors in neuronal migration and laminar organization of the cerebral cortex. Neuron 22, 277–289 (1999). [PubMed: 10069334]
47. Elices MJ, Urry LA, Hemler ME, Receptor functions for the integrin VLA-3: fibronectin, collagen, and laminin binding are differentially influenced by Arg-Gly-Asp peptide and by divalent cations. J Cell Biol 112, 169–181 (1991). [PubMed: 1986004]
48. Timpl R, Rohde H, Robey PG, Rennard SI, Foidart JM, Martin GR, Laminin--a glycoprotein from basement membranes. J Biol Chem 254, 9933–9937 (1979). [PubMed: 114518]
49. Nishiuchi R, Takagi J, Hayashi M, Ido H, Yagi Y, Sanzen N, Tsuji T, Yamada M, Sekiguchi K, Ligand-binding specificities of laminin-binding integrins: a comprehensive survey of laminin-integrin interactions using recombinant alpha3beta1, alpha6beta1, alpha7beta1 and alpha6beta4 integrins. Matrix Biol 25, 189–197 (2006). [PubMed: 16413178]
50. Choma DP, Milano V, Pumiglia KM, DiPersio CM, Integrin alpha3beta1-dependent activation of FAK/Src regulates Rac1-mediated keratinocyte polarization on laminin-5. J Invest Dermatol 127, 31–40 (2007). [PubMed: 16917494]
51. Kikkawa Y, Sanzen N, Sekiguchi K, Isolation and characterization of laminin-10/11 secreted by human lung carcinoma cells. laminin-10/11 mediates cell adhesion through integrin alpha3 beta1. J Biol Chem 273, 15854–15859 (1998). [PubMed: 9624186]

Author Manuscript Author Manuscript Author Manuscript Author Manuscript

52. Sime W, Lunderius-Andersson C, Enoksson M, Rousselle P, Tryggvason K, Nilsson G, Harvima I, Patarroyo M, Human mast cells adhere to and migrate on epithelial and vascular basement membrane laminins LM-332 and LM-511 via alpha3beta1 integrin. J Immunol 183, 4657–4665 (2009). [PubMed: 19752234]
53. Lerman YV, Lim K, Hyun YM, Falkner KL, Yang H, Pietropaoli AP, Sonnenberg A, Sarangi PP, Kim M, Sepsis lethality via exacerbated tissue infiltration and TLR-induced cytokine production by neutrophils is integrin alpha3beta1-dependent. Blood 124, 3515–3523 (2014). [PubMed: 25278585]
54. Desgrosellier JS, Cheresh DA, Integrins in cancer: biological implications and therapeutic opportunities. Nat Rev Cancer 10, 9–22 (2010). [PubMed: 20029421]
55. Subbaram S, Dipersio CM, Integrin alpha3beta1 as a breast cancer target. Expert Opin Ther Targets 15, 1197–1210 (2011). [PubMed: 21838596]
56. Tholmann S, Seebach J, Otani T, Florin L, Schnittler H, Gerke V, Furuse M, Ebnet K, JAM-A interacts with alpha3beta1 integrin and tetraspanins CD151 and CD9 to regulate collective cell migration of polarized epithelial cells. Cell Mol Life Sci 79, 88 (2022). [PubMed: 35067832]
57. Gorfu G, Virtanen I, Hukkanen M, Lehto VP, Rousselle P, Kenne E, Lindbom L, Kramer R, Tryggvason K, Patarroyo M, Laminin isoforms of lymph nodes and predominant role of alpha5-laminin(s) in adhesion and migration of blood lymphocytes. J Leukoc Biol 84, 701–712 (2008). [PubMed: 18523231]
58. Sixt M, Engelhardt B, Pausch F, Hallmann R, Wendler O, Sorokin LM, Endothelial cell laminin isoforms, laminins 8 and 10, play decisive roles in T cell recruitment across the blood-brain barrier in experimental autoimmune encephalomyelitis. J Cell Biol 153, 933–946 (2001). [PubMed: 11381080]
59. Carr TM, Wheaton JD, Houtz GM, Ciofani M, JunB promotes Th17 cell identity and restrains alternative CD4(+) T-cell programs during inflammation. Nat Commun 8, 301 (2017). [PubMed: 28824171]
60. Ciofani M, Madar A, Galan C, Sellars M, Mace K, Pauli F, Agarwal A, Huang W, Parkhurst CN, Muratet M, Newberry KM, Meadows S, Greenfield A, Yang Y, Jain P, Kirigin FK, Birchmeier C, Wagner EF, Murphy KM, Myers RM, Bonneau R, Littman DR, A validated regulatory network for Th17 cell specification. Cell 151, 289–303 (2012). [PubMed: 23021777]
61. Wu C, Ivars F, Anderson P, Hallmann R, Vestweber D, Nilsson P, Robenek H, Tryggvason K, Song J, Korpos E, Loser K, Beissert S, Georges-Labouesse E, Sorokin LM, Endothelial basement membrane laminin alpha5 selectively inhibits T lymphocyte extravasation into the brain. Nat Med 15, 519–527 (2009). [PubMed: 19396173]
62. Overstreet MG, Gaylo A, Angermann BR, Hughson A, Hyun YM, Lambert K, Acharya M, Billroth-Maclurg AC, Rosenberg AF, Topham DJ, Yagita H, Kim M, Lacy-Hulbert A, Meier-Schellersheim M, Fowell DJ, Inflammation-induced interstitial migration of effector CD4(+) T cells is dependent on integrin alphaV. Nat Immunol 14, 949–958 (2013). [PubMed: 23933892]
63. Glatigny S, Duhen R, Oukka M, Bettelli E, Cutting edge: loss of alpha4 integrin expression differentially affects the homing of Th1 and Th17 cells. J Immunol 187, 6176–6179 (2011). [PubMed: 22084440]
64. Hrastelj J, Andrews R, Loveless S, Morgan J, Bishop SM, Bray NJ, Williams NM, Robertson NP, CSF-resident CD4(+) T-cells display a distinct gene expression profile with relevance to immune surveillance and multiple sclerosis. Brain Commun 3, fcab155 (2021).
65. Kumar P, Monin L, Castillo P, Elsegeiny W, Horne W, Eddens T, Vikram A, Good M, Schoenborn AA, Bibby K, Montelaro RC, Metzger DW, Gulati AS, Kolls JK, Intestinal Interleukin-17 Receptor Signaling Mediates Reciprocal Control of the Gut Microbiota and Autoimmune Inflammation. Immunity 44, 659–671 (2016). [PubMed: 26982366]
66. Fabis MJ, Scott GS, Kean RB, Koprowski H, Hooper DC, Loss of blood-brain barrier integrity in the spinal cord is common to experimental allergic encephalomyelitis in knockout mouse models. Proc Natl Acad Sci U S A 104, 5656–5661 (2007). [PubMed: 17372191]
67. Song J, Wu C, Korpos E, Zhang X, Agrawal SM, Wang Y, Faber C, Schafers M, Korner H, Opdenakker G, Hallmann R, Sorokin L, Focal MMP-2 and MMP-9 activity at the blood-brain barrier promotes chemokine-induced leukocyte migration. Cell Rep 10, 1040–1054 (2015). [PubMed: 25704809]

Author Manuscript Author Manuscript Author Manuscript Author Manuscript

68. Hatfield JK, Brown MA, Group 3 innate lymphoid cells accumulate and exhibit disease-induced activation in the meninges in EAE. Cell Immunol 297, 69–79 (2015). [PubMed: 26163773]
69. Sutton CE, Lalor SJ, Sweeney CM, Brereton CF, Lavelle EC, Mills KH, Interleukin-1 and IL-23 induce innate IL-17 production from gammadelta T cells, amplifying Th17 responses and autoimmunity. Immunity 31, 331–341 (2009). [PubMed: 19682929]
70. Jager A, Dardalhon V, Sobel RA, Bettelli E, Kuchroo VK, Th1, Th17, and Th9 effector cells induce experimental autoimmune encephalomyelitis with different pathological phenotypes. J Immunol 183, 7169–7177 (2009). [PubMed: 19890056]
71. Zhong C, Cui K, Wilhelm C, Hu G, Mao K, Belkaid Y, Zhao K, Zhu J, Group 3 innate lymphoid cells continuously require the transcription factor GATA-3 after commitment. Nat Immunol 17, 169–178 (2016). [PubMed: 26595886]
72. Schlitzer A, McGovern N, Teo P, Zelante T, Atarashi K, Low D, Ho AW, See P, Shin A, Wasan PS, Hoeffel G, Malleret B, Heiseke A, Chew S, Jardine L, Purvis HA, Hilkens CM, Tam J, Poidinger M, Stanley ER, Krug AB, Renia L, Sivasankar B, Ng LG, Collin M, Ricciardi-Castagnoli P, Honda K, Haniffa M, Ginhoux F, IRF4 transcription factor-dependent CD11b+ dendritic cells in human and mouse control mucosal IL-17 cytokine responses. Immunity 38, 970–983 (2013). [PubMed: 23706669]
73. Persson EK, Uronen-Hansson H, Semmrich M, Rivollier A, Hagerbrand K, Marsal J, Gudjonsson S, Hakansson U, Reizis B, Kotarsky K, Agace WW, IRF4 transcription-factor-dependent CD103(+)CD11b(+) dendritic cells drive mucosal T helper 17 cell differentiation. Immunity 38, 958–969 (2013). [PubMed: 23664832]
74. Fooksman DR, Vardhana S, Vasiliver-Shamis G, Liese J, Blair DA, Waite J, Sacristan C, Victora GD, Zanin-Zhorov A, Dustin ML, Functional anatomy of T cell activation and synapse formation. Annu Rev Immunol 28, 79–105 (2010). [PubMed: 19968559]
75. Mittelbrunn M, Molina A, Escribese MM, Yanez-Mo M, Escudero E, Ursa A, Tejedor R, Mampaso F, Sanchez-Madrid F, VLA-4 integrin concentrates at the peripheral supramolecular activation complex of the immune synapse and drives T helper 1 responses. Proc Natl Acad Sci U S A 101, 11058–11063 (2004). [PubMed: 15263094]
76. Kandula S, Abraham C, LFA-1 on CD4+ T cells is required for optimal antigen-dependent activation in vivo. J Immunol 173, 4443–4451 (2004). [PubMed: 15383575]
77. Bonilha CS, Benson RA, Scales HE, Brewer JM, Garside P, Junctional adhesion molecule-A on dendritic cells regulates Th1 differentiation. Immunol Lett 235, 32–40 (2021). [PubMed: 34000305]
78. Hood JD, Cheresh DA, Role of integrins in cell invasion and migration. Nat Rev Cancer 2, 91–100 (2002). [PubMed: 12635172]
79. Mangan PR, Harrington LE, O'Quinn DB, Helms WS, Bullard DC, Elson CO, Hatton RD, Wahl SM, Schoeb TR, Weaver CT, Transforming growth factor-beta induces development of the T(H)17 lineage. Nature 441, 231–234 (2006). [PubMed: 16648837]
80. Li L, Shi QG, Lin F, Liang YG, Sun LJ, Mu JS, Wang YG, Su HB, Xu B, Ji CC, Huang HH, Li K, Wang HF, Cytokine IL-6 is required in Citrobacter rodentium infection-induced intestinal Th17 responses and promotes IL-22 expression in inflammatory bowel disease. Mol Med Rep 9, 831–836 (2014). [PubMed: 24430732]
81. Alon R, Ley K, Cells on the run: shear-regulated integrin activation in leukocyte rolling and arrest on endothelial cells. Curr Opin Cell Biol 20, 525–532 (2008). [PubMed: 18499427]
82. Lee JW, Juliano R, Mitogenic signal transduction by integrin- and growth factor receptor-mediated pathways. Mol Cells 17, 188–202 (2004). [PubMed: 15179030]
83. Larochelle C, Uphaus T, Broux B, Gowing E, Paterka M, Michel L, Dudvarski Stankovic N, Bicker F, Lemaitre F, Prat A, Schmidt MHH, Zipp F, EGFL7 reduces CNS inflammation in mouse. Nat Commun 9, 819 (2018). [PubMed: 29483510]
84. Schraml BU, Hildner K, Ise W, Lee WL, Smith WA, Solomon B, Sahota G, Sim J, Mukasa R, Cemerski S, Hatton RD, Stormo GD, Weaver CT, Russell JH, Murphy TL, Murphy KM, The AP-1 transcription factor Batf controls T(H)17 differentiation. Nature 460, 405–409 (2009). [PubMed: 19578362]

Author Manuscript Author Manuscript Author Manuscript Author Manuscript

85. Brustle A, Heink S, Huber M, Rosenplanter C, Stadelmann C, Yu P, Arpaia E, Mak TW, Kamradt T, Lohoff M, The development of inflammatory T(H)-17 cells requires interferon-regulatory factor 4. Nat Immunol 8, 958–966 (2007). [PubMed: 17676043]

86. Yang XO, Panopoulos AD, Nurieva R, Chang SH, Wang D, Watowich SS, Dong C, STAT3 regulates cytokine-mediated generation of inflammatory helper T cells. J Biol Chem 282, 9358–9363 (2007). [PubMed: 17277312]

87. Ivanov II, McKenzie BS, Zhou L, Tadokoro CE, Lepelley A, Lafaille JJ, Cua DJ, Littman DR, The orphan nuclear receptor RORgammat directs the differentiation program of proinflammatory IL-17+ T helper cells. Cell 126, 1121–1133 (2006). [PubMed: 16990136]

88. Yoon JH, Sudo K, Kuroda M, Kato M, Lee IK, Han JS, Nakae S, Imamura T, Kim J, Ju JH, Kim DK, Matsuzaki K, Weinstein M, Matsumoto I, Sumida T, Mamura M, Phosphorylation status determines the opposing functions of Smad2/Smad3 as STAT3 cofactors in TH17 differentiation. Nat Commun 6, 7600 (2015). [PubMed: 26194464]

89. Martinez GJ, Zhang Z, Chung Y, Reynolds JM, Lin X, Jetten AM, Feng XH, Dong C, Smad3 differentially regulates the induction of regulatory and inflammatory T cell differentiation. J Biol Chem 284, 35283–35286 (2009). [PubMed: 19887374]

90. Veldhoen M, Hocking RJ, Flavell RA, Stockinger B, Signals mediated by transforming growth factor-beta initiate autoimmune encephalomyelitis, but chronic inflammation is needed to sustain disease. Nat Immunol 7, 1151–1156 (2006). [PubMed: 16998492]

91. Li MO, Wan YY, Flavell RA, T cell-produced transforming growth factor-beta1 controls T cell tolerance and regulates Th1- and Th17-cell differentiation. Immunity 26, 579–591 (2007). [PubMed: 17481928]

92. Iezzi G, Sonderegger I, Ampenberger F, Schmitz N, Marsland BJ, Kopf M, CD40-CD40L cross-talk integrates strong antigenic signals and microbial stimuli to induce development of IL-17-producing CD4+ T cells. Proc Natl Acad Sci U S A 106, 876–881 (2009). [PubMed: 19136631]

93. Gomez-Rodriguez J, Wohlfert EA, Handon R, Meylan F, Wu JZ, Anderson SM, Kirby MR, Belkaid Y, Schwartzberg PL, Itk-mediated integration of T cell receptor and cytokine signaling regulates the balance between Th17 and regulatory T cells. J Exp Med 211, 529–543 (2014). [PubMed: 24534190]

94. Harjunpaa H, Llort Asens M, Guenther C, Fagerholm SC, Cell Adhesion Molecules and Their Roles and Regulation in the Immune and Tumor Microenvironment. Front Immunol 10, 1078 (2019). [PubMed: 31231358]

95. Yazlovitskaya EM, Tseng HY, Viquez O, Tu T, Mernaugh G, McKee KK, Riggins K, Quaranta V, Pathak A, Carter BD, Yurchenco P, Sonnenberg A, Bottcher RT, Pozzi A, Zent R, Integrin alpha3beta1 regulates kidney collecting duct development via TRAF6-dependent K63-linked polyubiquitination of Akt. Mol Biol Cell 26, 1857–1874 (2015). [PubMed: 25808491]

96. Jakus Z, Fodor S, Abram CL, Lowell CA, Mocsai A, Immunoreceptor-like signaling by beta 2 and beta 3 integrins. Trends Cell Biol 17, 493–501 (2007). [PubMed: 17913496]

97. Woodside DG, Obergfell A, Talapatra A, Calderwood DA, Shattil SJ, Ginsberg MH, The N-terminal SH2 domains of Syk and ZAP-70 mediate phosphotyrosine-independent binding to integrin beta cytoplasmic domains. J Biol Chem 277, 39401–39408 (2002). [PubMed: 12171941]

98. Lin TH, Rosales C, Mondal K, Bolen JB, Haskill S, Juliano RL, Integrin-mediated tyrosine phosphorylation and cytokine message induction in monocytic cells. A possible signaling role for the Syk tyrosine kinase. J Biol Chem 270, 16189–16197 (1995). [PubMed: 7541794]

99. Sobocinski GP, Toy K, Bobrowski WF, Shaw S, Anderson AO, Kaldjian EP, Ultrastructural localization of extracellular matrix proteins of the lymph node cortex: evidence supporting the reticular network as a pathway for lymphocyte migration. BMC Immunol 11, 42 (2010). [PubMed: 20716349]

100. Zhang X, Wang Y, Song J, Gerwien H, Chuquisana O, Chashchina A, Denz C, Sorokin L, The endothelial basement membrane acts as a checkpoint for entry of pathogenic T cells into the brain. J Exp Med 217, (2020).

Author Manuscript Author Manuscript Author Manuscript Author Manuscript

101. Heng AHS, Han CW, Abbott C, McColl SR, Comerford I, Chemokine-Driven Migration of Pro-Inflammatory CD4(+) T Cells in CNS Autoimmune Disease. Front Immunol 13, 817473 (2022). [PubMed: 35250997]
102. Rosenthal KM, Edwards LJ, Sabatino JJ Jr., Hood JD, Wasserman HA, Zhu C, Evavold BD, Low 2-dimensional CD4 T cell receptor affinity for myelin sets in motion delayed response kinetics. PLoS One 7, e32562 (2012). [PubMed: 22412888]
103. Daneman R, Rescigno M, The gut immune barrier and the blood-brain barrier: are they so different? Immunity 31, 722–735 (2009). [PubMed: 19836264]
104. Kurmaeva E, Lord JD, Zhang S, Bao JR, Kevil CG, Grisham MB, Ostanin DV, T cell-associated alpha4beta7 but not alpha4beta1 integrin is required for the induction and perpetuation of chronic colitis. Mucosal Immunol 7, 1354–1365 (2014). [PubMed: 24717354]
105. Dotan I, Allez M, Danese S, Keir M, Tole S, McBride J, The role of integrins in the pathogenesis of inflammatory bowel disease: Approved and investigational anti-integrin therapies. Med Res Rev 40, 245–262 (2020). [PubMed: 31215680]
106. Stenstad H, Ericsson A, Johansson-Lindbom B, Svensson M, Marsal J, Mack M, Picarella D, Soler D, Marquez G, Briskin M, Agace WW, Gut-associated lymphoid tissue-primed CD4+ T cells display CCR9-dependent and -independent homing to the small intestine. Blood 107, 3447–3454 (2006). [PubMed: 16391017]
107. Bauche D, Marie JC, Transforming growth factor beta: a master regulator of the gut microbiota and immune cell interactions. Clin Transl Immunology 6, e136 (2017). [PubMed: 28523126]
108. Ammon C, Meyer SP, Schwarzfischer L, Krause SW, Andreesen R, Kreutz M, Comparative analysis of integrin expression on monocyte-derived macrophages and monocyte-derived dendritic cells. Immunology 100, 364–369 (2000). [PubMed: 10929059]
109. Domingues HS, Mues M, Lassmann H, Wekerle H, Krishnamoorthy G, Functional and pathogenic differences of Th1 and Th17 cells in experimental autoimmune encephalomyelitis. PLoS One 5, e15531 (2010). [PubMed: 21209700]
110. Bolger AM, Lohse M, Usadel B, Trimmomatic: a flexible trimmer for Illumina sequence data. Bioinformatics 30, 2114–2120 (2014). [PubMed: 24695404]
111. Dobin A, Davis CA, Schlesinger F, Drenkow J, Zaleski C, Jha S, Batut P, Chaisson M, Gingeras TR, STAR: ultrafast universal RNA-seq aligner. Bioinformatics 29, 15–21 (2013). [PubMed: 23104886]
112. Harrow J, Frankish A, Gonzalez JM, Tapanari E, Diekhans M, Kokocinski F, Aken BL, Barrell D, Zadissa A, Searle S, Barnes I, Bignell A, Boychenko V, Hunt T, Kay M, Mukherjee G, Rajan J, Despacio-Reyes G, Saunders G, Steward C, Harte R, Lin M, Howald C, Tanzer A, Derrien T, Chrast J, Walters N, Balasubramanian S, Pei B, Tress M, Rodriguez JM, Ezkurdia I, van Baren J, Brent M, Haussler D, Kellis M, Valencia A, Reymond A, Gerstein M, Guigo R, Hubbard TJ, GENCODE: the reference human genome annotation for The ENCODE Project. Genome Res 22, 1760–1774 (2012). [PubMed: 22955987]
113. Liao Y, Smyth GK, Shi W, The Subread aligner: fast, accurate and scalable read mapping by seed-and-vote. Nucleic Acids Res 41, e108 (2013). [PubMed: 23558742]
114. Love MI, Huber W, Anders S, Moderated estimation of fold change and dispersion for RNA-seq data with DESeq2. Genome Biol 15, 550 (2014). [PubMed: 25516281]
115. Zhu A, Ibrahim JG, Love MI, Heavy-tailed prior distributions for sequence count data: removing the noise and preserving large differences. Bioinformatics 35, 2084–2092 (2019). [PubMed: 30395178]
116. Li B, Dewey CN, RSEM: accurate transcript quantification from RNA-Seq data with or without a reference genome. BMC Bioinformatics 12, 323 (2011). [PubMed: 21816040]

Author Manuscript Author Manuscript Author Manuscript Author Manuscript

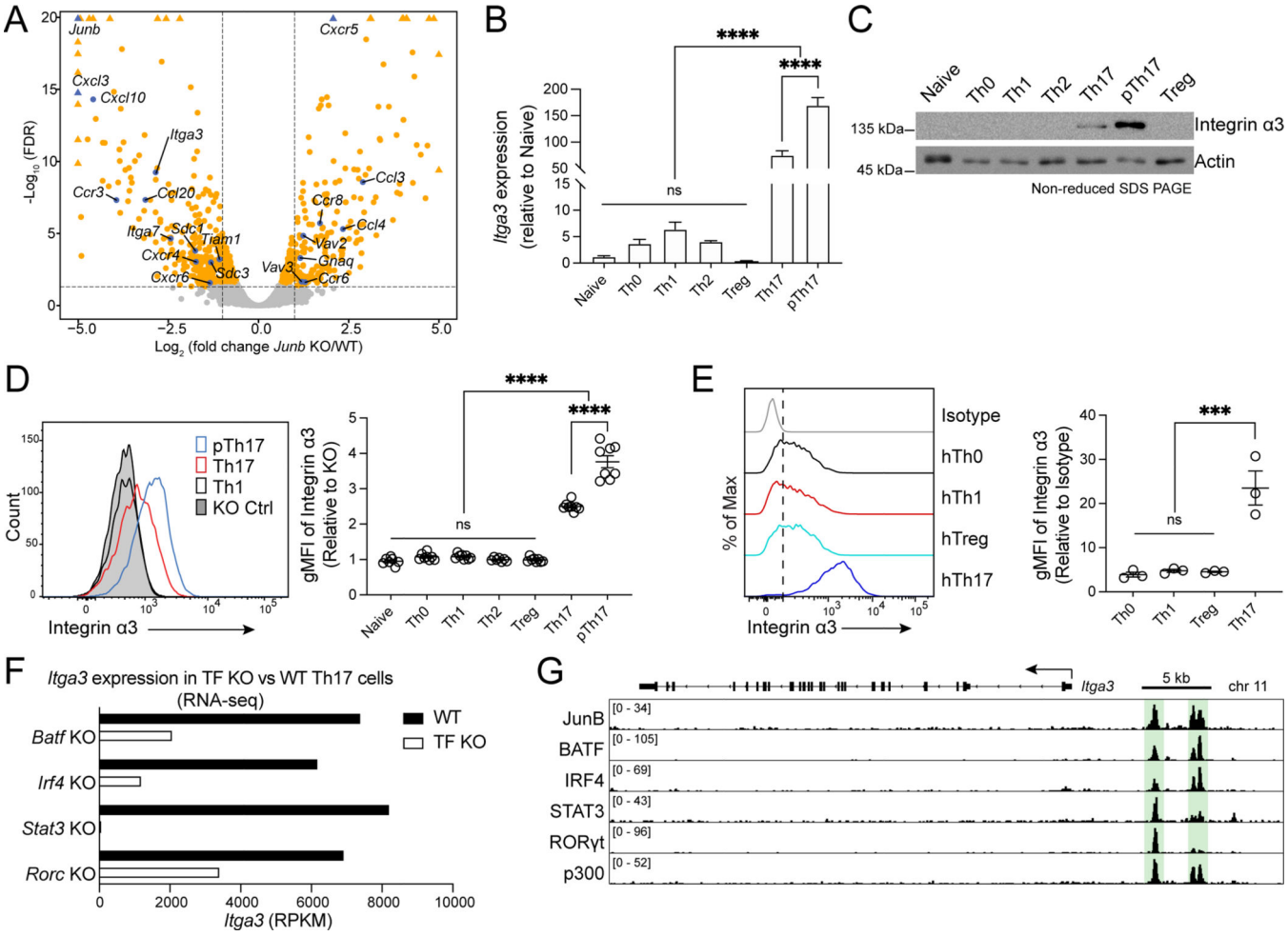

Fig. 1. Integrin α3 is exclusively expressed by Th17 cells.

(A) Volcano plot showing DEGs in *Junb*$^{+/+}$ *CD4-Cre* (WT) and *Junb*$^{fl/fl}$ *CD4-Cre* (*Junb* KO) Th17 cells polarized *in vitro* for 48 h. Genes with FC > 2 and FDR < 0.05 are in orange, and select migration-related genes are labeled and highlighted in blue. Triangles indicate genes with FDR < 10^{-20} or Log_2(FC) > 5 or < −5. Expression of integrin α3 in 72 h polarization cultures was detected by **(B)** qPCR (n = 4 mice/subset, pooled from 3 independent experiments), **(C)** Western blot (representative of 3 independent experiments), and **(D)** flow cytometry (n = 7–8 mice/subset, pooled from 4 independent experiments). KO Ctrl, negative staining control is *Itga3*-deficient Th1 culture (*Itga3*$^{fl/fl}$ *CD4-Cre*). mRNA expression is presented relative to *Actb* expression and normalized over naïve CD4$^+$ T cells. **(E)** Integrin α3 expression for day 6 cultures of human (h) naïve CD4$^+$ T cells polarized as indicated. n = 3 donors/subset, pooled from 3 independent experiments. **(F)** Bar plot of RPKM expression values of *Itga3* transcripts in TF-knock-out (TF KO, *Batf*$^{-/-}$, *Irf4*$^{-/-}$, *Stat3*$^{fl/fl}$ *CD4-Cre*, *Rorc(t)*$^{GFP/GFP}$) vs wild-type (WT) 48 h Th17 cell polarization cultures (differential expression, FDR < 10^{-5}). **(G)** ChIP-seq tracks for TFs and p300 peaks enriched at *Itga3*-proximal putative enhancers (shaded green) in 48 h Th17 cell cultures. gMFI presented as fold over Naïve (D) or Isotype (E). Data are summarized as mean ± SEM.

One-way ANOVA test. *, $p < 0.05$; **, $p < 0.01$; ***, $p < 0.001$; ****, $p < 0.0001$; ns, not significant. Datasets for (f) and (g) from GSE40918 and GSE98414.

Author Manuscript Author Manuscript Author Manuscript Author Manuscript

Author Manuscript Author Manuscript Author Manuscript Author Manuscript

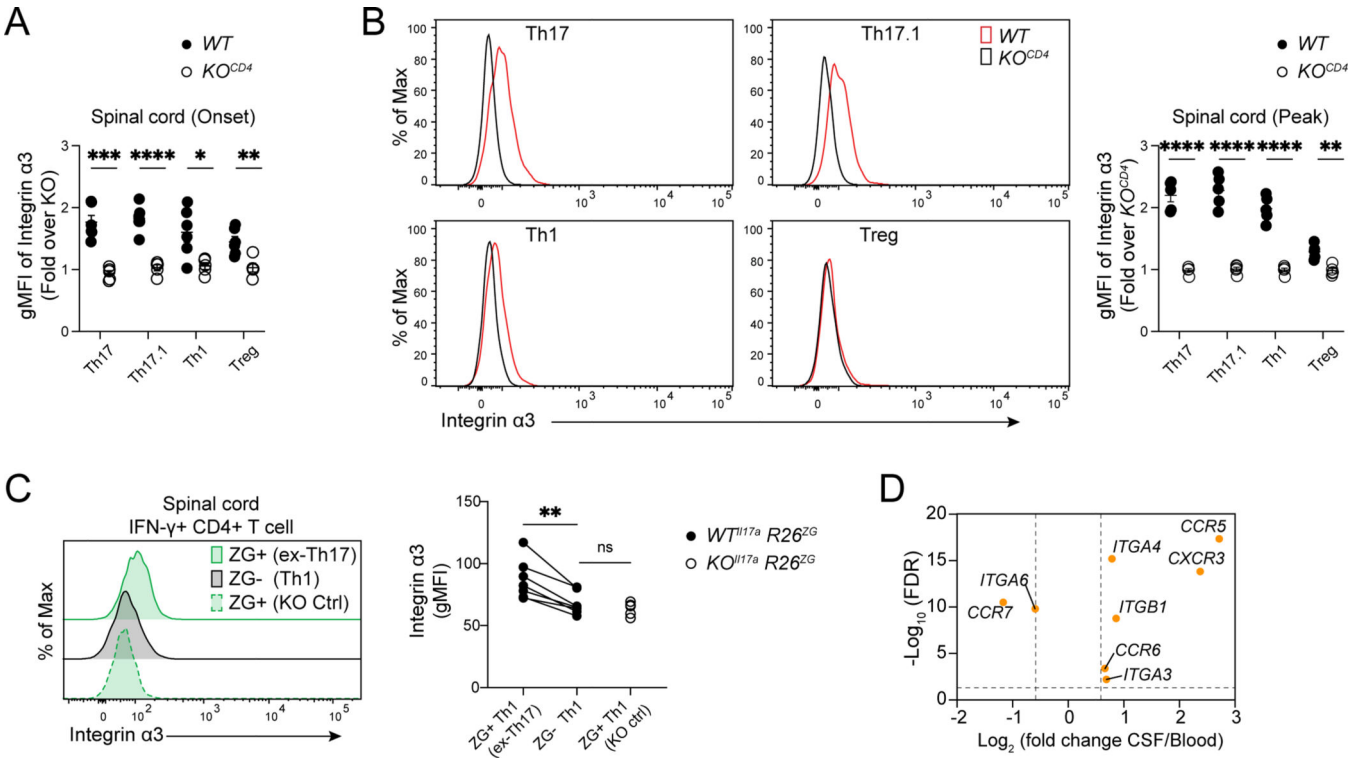

Fig. 2. CNS-infiltrating Th17 cells express integrin α3 during EAE pathogenesis.

Flow cytometric analysis of integrin α3 expression on CD4$^+$ T cell subsets isolated from the spinal cord of EAE-induced ***Itga3*$^{fl/fl}$ CD4-Cre (*KO*^{CD4}) or wildtype control mice (A)** at the onset (day 13, n = 5–6 mice/genotype) or **(B)** at the peak (day 14, n = 5 mice/genotype). CD4$^+$ T cell subsets: Th17, IL-17A$^+$ IFN-γ$^-$; Th17.1, IL-17A$^+$ IFN-γ$^+$; Th1, IL-17A$^-$ IFN-γ$^+$; Treg, IL-17A$^-$ Foxp3$^+$. **(C)** Flow cytometric analysis of integrin α3 expression on ZG$^+$ or ZG$^-$ IFN-γ-producing CD4$^+$ T cells isolated from the spinal cord of *WT*^{Il17a} *R26*^{ZG} or *KO*^{Il17a} *R26*^{ZG} (KO Ctrl) mice at the peak of EAE (day 17, n = 5–6 mice/genotype). EAE inductions in **(A**, **B**, and **C)** were performed independently, once with biological replicates. **(D)** Plot showing select migration-related DEGs in CSF CD4$^+$ T cells versus blood CD4$^+$ T cells from MS patients. Dashed lines represent FDR = 0.05 and fold change = −1.5 or 1.5. RNA-seq data is replotted from (64). gMFI presented as fold over KO (**A** and **B**). Data are summarized as mean ± SEM (**A** and **B**) or represented by lines connecting data from the same mouse (**C**). Unpaired Student's *t*-test (**A**, **B**, and **C**) and paired Student's *t*-test (**C**). *, $p < 0.05$; **, $p < 0.01$; ***, $p < 0.001$; ns, not significant.

Author Manuscript Author Manuscript Author Manuscript Author Manuscript

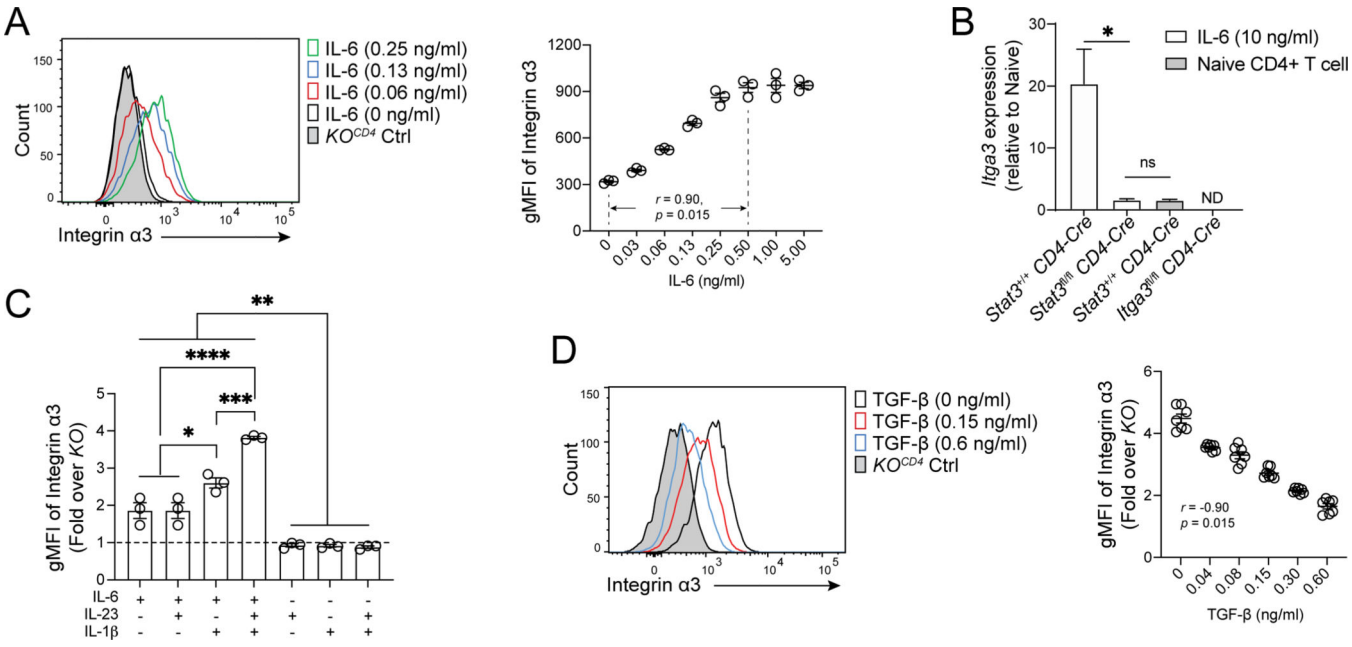

Fig. 3. Integrin α3 expression is induced by the IL-6-Stat3 pathway.

(A) Flow cytometric analysis of integrin α3 expression by CD4$^+$ T cells cultured for 72 h in the presence of IL-6 (0–5.0 ng/ml). *n* = 3 mice, representative of 3 independent experiments. **(B)** qPCR analysis of *Itga3* transcript in *Stat3*$^{+/+}$ *CD4-Cre* and *Stat3*$^{fl/fl}$ *CD4-Cre* naïve CD4$^+$ T cells cultured for 18 h in the presence of IL-6 (10 ng/ml). Naïve CD4$^+$ T cells from *Itga3*$^{fl/fl}$ *CD4-Cre* mice serve as a negative *Itga3* control. mRNA expression is presented relative to *Actb* expression and normalized over *Stat3*$^{+/+}$ *CD4-Cre* naïve CD4$^+$ T cells (Naïve). *n* = 4 mice/genotype, pooled from 3 independent experiments. ND, not detectable. **(C)** Flow cytometric analysis of integrin α3 in naïve CD4$^+$ T cells cultured for 72 h in the presence of indicated cytokines (IL-6, 10 ng/ml; IL-1β, 20 ng/ml; IL-23, 25 ng/ml). *n* = 3 mice, representative of 3 independent experiments. **(D)** Flow cytometric analysis of integrin α3 expression in pTh17 cells cultured for 72 h in the presence of TGF-β (0–0.6 ng/ml). *n* = 7 mice, pooled from 2 independent experiments. *r*, Pearson's correlation coefficient calculated for cultures treated with 0–0.5 ng/mL of IL-6 **(A)** and with 0–0.6 ng/mL of TGF-β **(D)**. Naïve CD4$^+$ T cells isolated from *Itga3*$^{fl/fl}$ *CD4-Cre* mice and cultured without cytokines served as a negative staining control (*KO*^{CD4} Ctrl) **(A and D)**. gMFI presented as fold over *KO*^{CD4} cells cultured under identical conditions **(A, C, and D)**. Data are summarized as mean ± SEM. Unpaired Student's *t*-test **(B)** or one-way ANOVA test **(C)**. *, $p < 0.05$; **, $p < 0.01$; ***, $p < 0.001$; ns, not significant.

Author Manuscript Author Manuscript Author Manuscript Author Manuscript

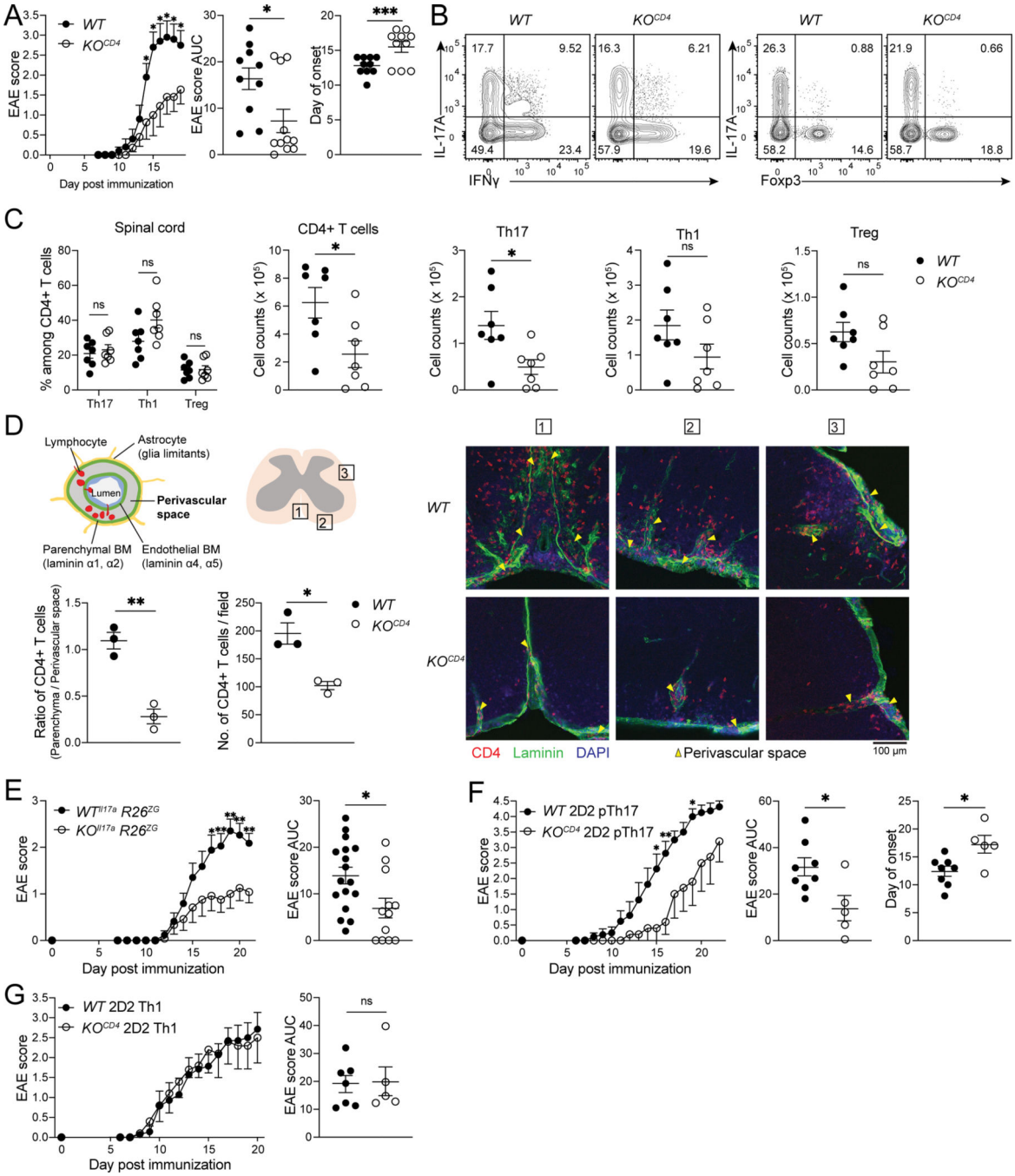

Fig. 4. Deletion of integrin α3 in CD4$^+$ T cells attenuates EAE.

(A) Clinical score of EAE from *WT* ($n = 10$) and *KO^{CD4}* ($n = 11$) mice, pooled from 2 independent experiments. The area under the curve (AUC) values calculated from EAE clinical scores were compared. **(B)** Representative flow cytometric analysis of CD4$^+$ T cells isolated from the spinal cords of EAE-induced mice at disease peak (day 16). **(C)** The frequencies and numbers of CD4$^+$ T cell subsets in the spinal cords of EAE-induced mice at disease peak (day 16, $n = 5$–6 mice/genotype, representative of 2 independent experiments). CD4$^+$ T cell subsets: Th17, IL-17A$^+$; Th1, IFN-γ$^+$; Treg, Foxp3$^+$. **(D)** Spinal

Author Manuscript Author Manuscript Author Manuscript Author Manuscript

cord infiltration of $CD4^+$ T cells at disease peak (day 16) imaged by confocal microscopy. $n = 3$ mice/genotype, representative of 2 independent experiments. (Left) Schematic image of perivascular cuff depicts the accumulation of leukocytes in the perivascular space between basement membranes. The perivascular space is surrounded by the endothelial and the parenchymal basement membranes that are visualized by pan-laminin (green). (Right) Representative immunofluorescence images selected from three different regions of spinal cord sections. CD4, red; pan-laminin, green. Perivascular spaces in the immunofluorescence images are marked by yellow arrowheads. **(E)** Clinical score of EAE from WT^{Il17a} $R26^{ZG}$ ($n = 17$) and KO^{Il17a} $R26^{ZG}$ mice ($n = 12$) mice, pooled from 2 independent experiments. **(F)** Clinical score of passive EAE induced by adoptive transfer of *in vitro* cultured *WT* or KO^{CD4} 2D2 pTh17 cells into $Tcra^{-/-}$ mice (*WT* pTh17 cells, $n = 8$; KO^{CD4} pTh17 cells, $n = 5$, representative of 2 independent experiments). **(G)** Clinical score of passive EAE induced by adoptive transfer of *in vitro* cultured *WT* or KO^{CD4} 2D2 Th1 cells into $Tcra^{-/-}$ mice (*WT* Th1 cells, $n = 7$; KO^{CD4} Th1 cells, $n = 5$, representative of 2 independent experiments). Data are summarized as mean ± SEM. Mann-Whitney *U*-test or Unpaired Student's *t*-test **(D)**. *, $p < 0.05$; **, $p < 0.01$; ***, $p < 0.001$; ns, not significant.

Author Manuscript Author Manuscript Author Manuscript Author Manuscript

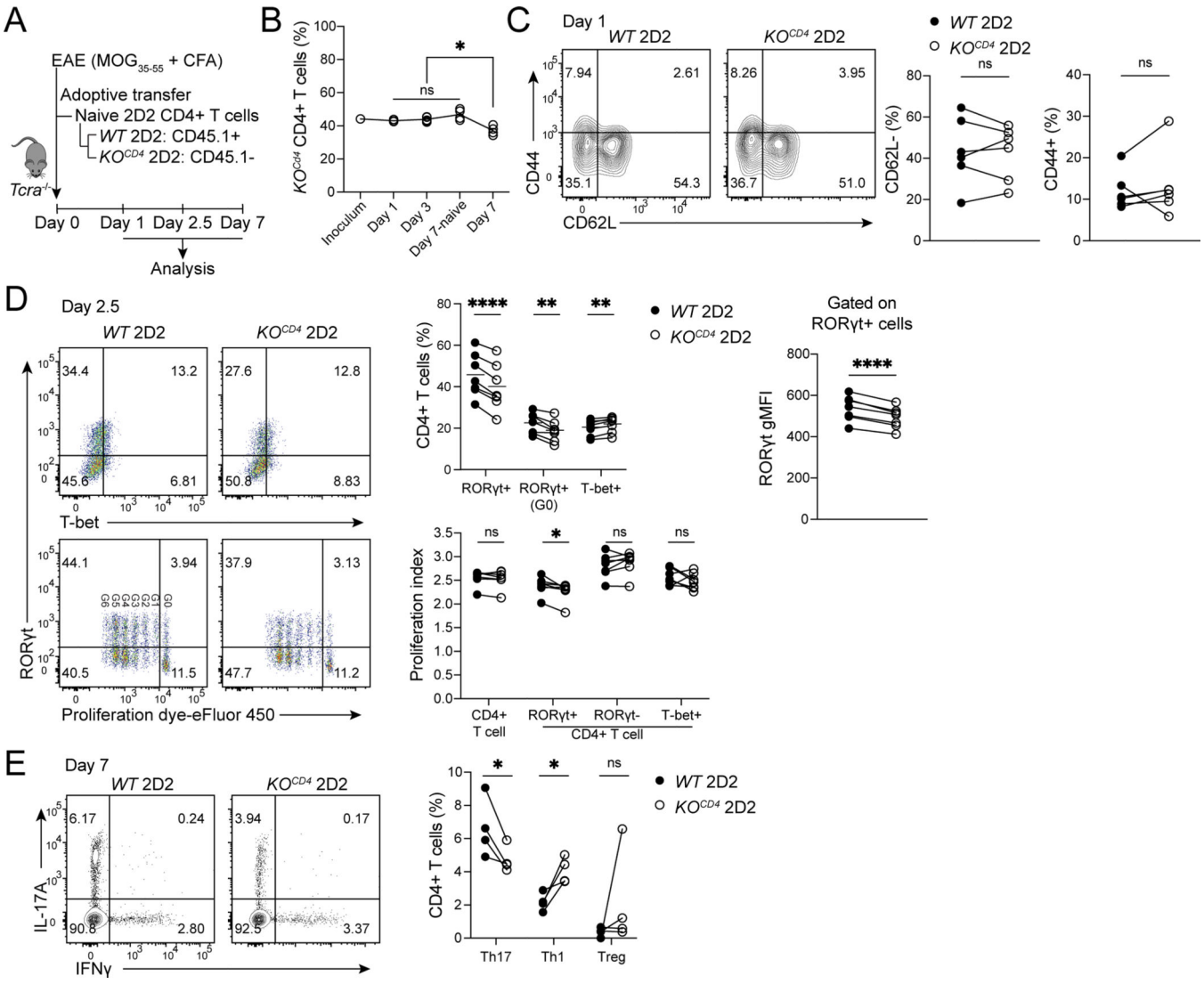

Fig. 5. Integrin α3 is required for the polarization and expansion of Th17 cells *in vivo*.

(A) Schematic of EAE induction in *Tcra*$^{-/-}$ mice and adoptive transfer of naïve CD4$^+$ T cells. Naïve CD4$^+$ T cells obtained from *WT* 2D2 (CD45.1$^+$) and *KO*^{CD4} 2D2 (CD45.1$^-$) mice were mixed at a 1:1 ratio and adoptively transferred into EAE-induced *Tcra*$^{-/-}$ mice. CD4$^+$ T cells were loaded with proliferation dye prior to the adoptive transfer. CD4$^+$ T cells in iLNs were analyzed at **(C)** 24 h, **(D)** 60 h, and **(E)** 7 days post EAE induction. **(B)** Plot showing the percentage of *KO*^{CD4} 2D2 CD4$^+$ T cells within total CD4$^+$ T cells in iLNs of EAE-induced or naïve *Tcra*$^{-/-}$ mice. $n = 3–4$ mice, representative of 2 independent experiments. **(C)** Flow cytometric analysis of CD62L and CD44 expression on CD4$^+$ T cells isolated from iLNs of *Tcra*$^{-/-}$ mice at 24 h post EAE induction. $n = 6$ mice, pooled from 2 independent experiments. **(D)** Flow cytometric analysis of TF expression in CD4$^+$ T cells isolated from iLNs of *Tcra*$^{-/-}$ mice at 2.5 days post EAE induction. $n = 7$ mice, representative of 2 independent experiments. Horizontal lines indicate mean values. G0–6, generations 0–6. **(E)** Flow cytometric analysis of CD4$^+$ T cells isolated from iLNs of *Tcra*$^{-/-}$ mice at 7 days post EAE induction. $n = 4$ mice, representative of 2 independent experiments.

Author Manuscript Author Manuscript Author Manuscript Author Manuscript

$CD4^+$ T cell subsets: Th17, IL-$17A^+$; Th1, IFN-γ^+; Treg, $Foxp3^+$. Data are summarized as mean ± SEM. Mean values **(B)** or data acquired from the same recipient mouse **(C-E)** are connected by lines. One-way ANOVA test **(B)** and paired Student's *t*-test **(C-E)**. *, $p < 0.05$; **, $p < 0.01$; ****, $p < 0.0001$; ns, not significant.

Author Manuscript Author Manuscript Author Manuscript Author Manuscript

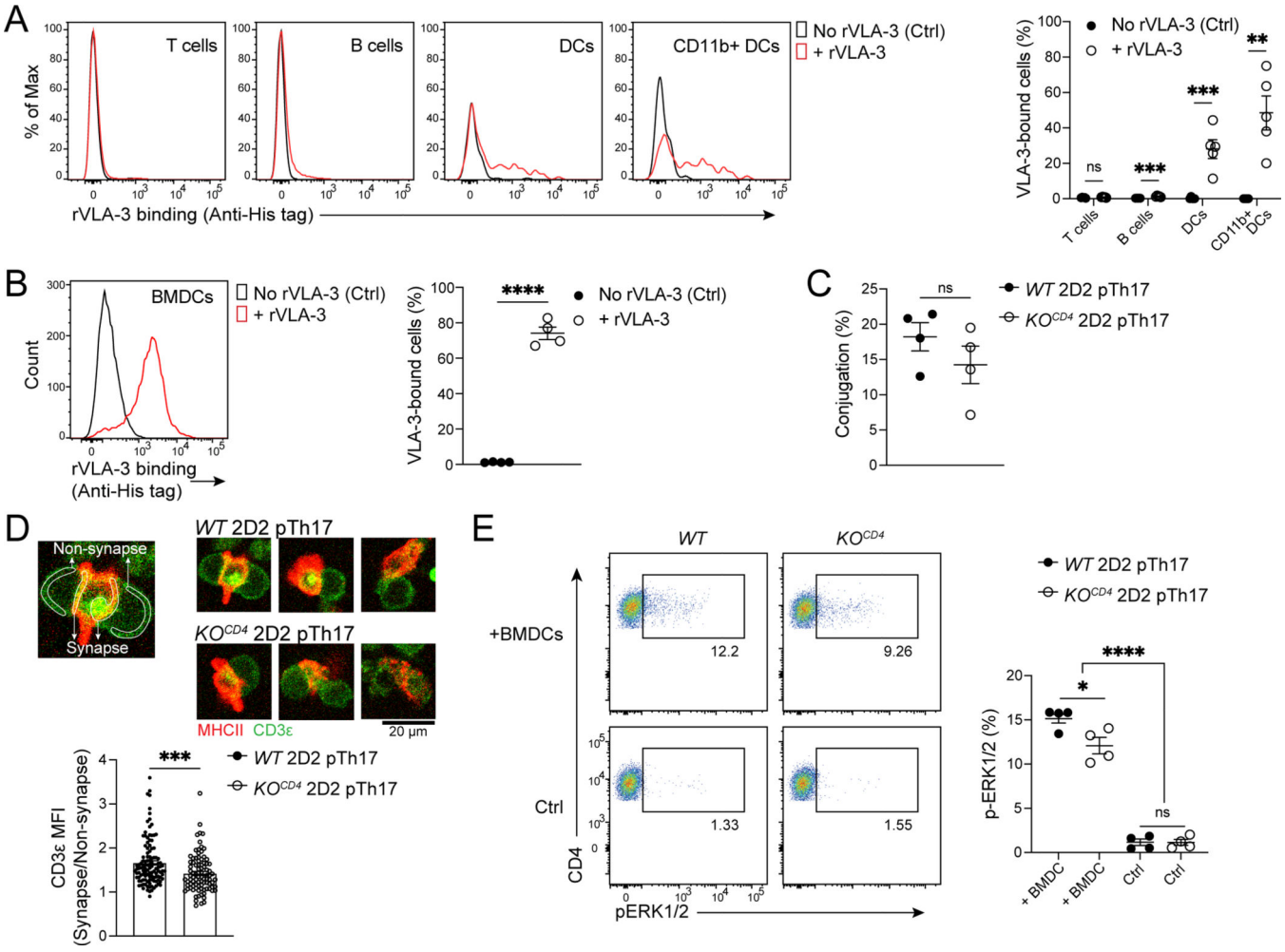

Fig. 6. Integrin α3 promotes T cell stimulation by facilitating T cell-APC interaction.

Flow cytometric analysis of recombinant integrin α3β1 (rVLA-3) binding to **(A)** cells isolated from iLNs of EAE-induced mice (day 7, $n = 5$ mice, representative 2 independent experiments) or **(B)** CD11c$^+$ BMDCs ($n = 4$ mice, pooled from 2 independent experiments). T cells, MHCII$^-$ CD3ε$^+$; B cells, MHCII$^+$ CD3ε$^-$ CD19$^+$; Dendritic cells, MHCII$^+$ CD3ε$^-$ CD19$^-$ CD11c$^+$. Cells incubated without rVLA-3 were used as a negative staining control (Ctrl). *WT* or *KO^{CD4}* 2D2 pTh17 cells were co-cultured with $MOG_{35–55}$ peptide-pulsed BMDCs for 30 min **(C and D)** or 5 min **(E)**. **(C)** The percentage of 2D2 pTh17 cells making conjugations with BMDCs. $n = 3$ mice/genotype, pooled from 3 independent experiments. **(D)** The immunological synapse formation between 2D2 pTh17 cells and BMDCs (*WT* 2D2 pTh17 cells, $n = 115$; *KO^{CD4}* 2D2 pTh17 cells, $n = 90$, pooled from 4 independent experiments). **(E)** Flow cytometric analysis of p-ERK1/2 in 2D2 pTh17 cells. Pooled from 4 independent experiments. Data are summarized as mean ± SEM. Unpaired Student's *t*-test **(A-D)** or two-way ANOVA test **(E)**. *, $p < 0.05$; **, $p < 0.01$; ***, $p < 0.001$; ****, $p < 0.0001$; ns, not significant.

Author Manuscript Author Manuscript Author Manuscript Author Manuscript

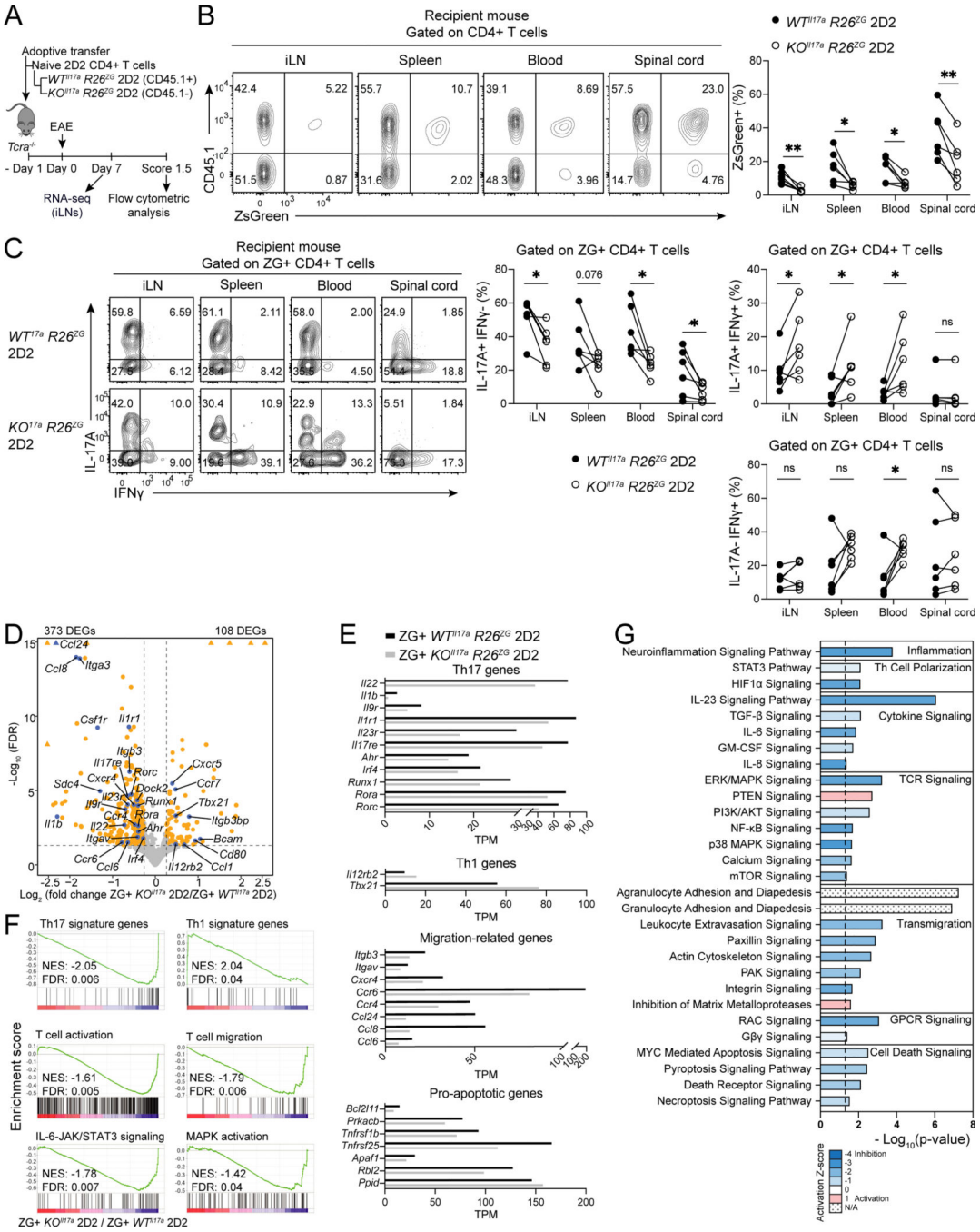

Fig. 7. Integrin α3 promotes the maintenance of Th17 cell identity.

(A) Schematic of EAE induction in *Tcra*$^{-/-}$ mice post adoptive transfer of naïve CD4^{+} T cells. Naïve CD4^{+} T cells obtained from *WT*^{Il17a} *R26*^{ZG} 2D2 (CD45.1^{+}) and *KO*^{Il17a} *R26*^{ZG} 2D2 (CD45.1^{-}) mice were mixed at a 1:1 ratio and adoptively transferred into *Tcra*$^{-/-}$ mice. EAE was induced on the following day. Organs were harvested at clinical score of 1.5 for the analysis of frequency and cytokine expression profiles of ZG^{+} cells **(B-C)**. 7 days post immunization, ZG^{+} *WT*^{Il17a} 2D2 or ZG^{+} *KO*^{Il17a} 2D2 cells were FACS-sorted from iLNs to perform RNA-seq **(D-G)**. **(B)** The frequency of ZG^{+} populations in CD4^{+} T cells of each

Author Manuscript Author Manuscript Author Manuscript Author Manuscript

genotype was analyzed for indicated tissues. $n = 6$ mice, representative of 2 independent experiments. **(C)** Cytokine expression profiles of ZG^+ $CD4^+$ T cells of each genotype were analyzed for indicated tissues. $n = 6$ mice, representative of 2 independent experiments. **(D)** Volcano plot showing DEGs in ZG^+ KO^{Il17a} 2D2 vs ZG^+ WT^{Il17a} 2D2 RNA-seq analysis. Genes considered significant (FC > 1.2 and FDR < 0.05) are in orange, and select genes are labeled and highlighted in blue. FDR capped at 10^{-15}. Log_2 (FC) capped at −2.5 or 2.5. Triangles indicate genes with FDR < 10^{-15} or Log_2 (FC) > 2.5 or < −2.5. **(E)** Bar plots showing the RNA-seq expression level (TPM) of select genes. **(F)** GSEA plots enriched in various gene sets for ranked genes in ZG^+ KO^{Il17a} 2D2 vs ZG^+ WT^{Il17a} 2D2 RNA-seq. **(G)** Ingenuity pathway analysis for DEGs (FDR < 0.05) in ZG^+ KO^{Il17a} 2D2 vs ZG^+ WT^{Il17a} 2D2 RNA-seq. Dashed line represents p-value = 0.05. Data acquired from the same recipient mouse are connected by lines (B and C). Paired Student's t-test (B and C). *, $p < 0.05$; **, $p < 0.01$; ns, not significant.

Author Manuscript Author Manuscript Author Manuscript Author Manuscript

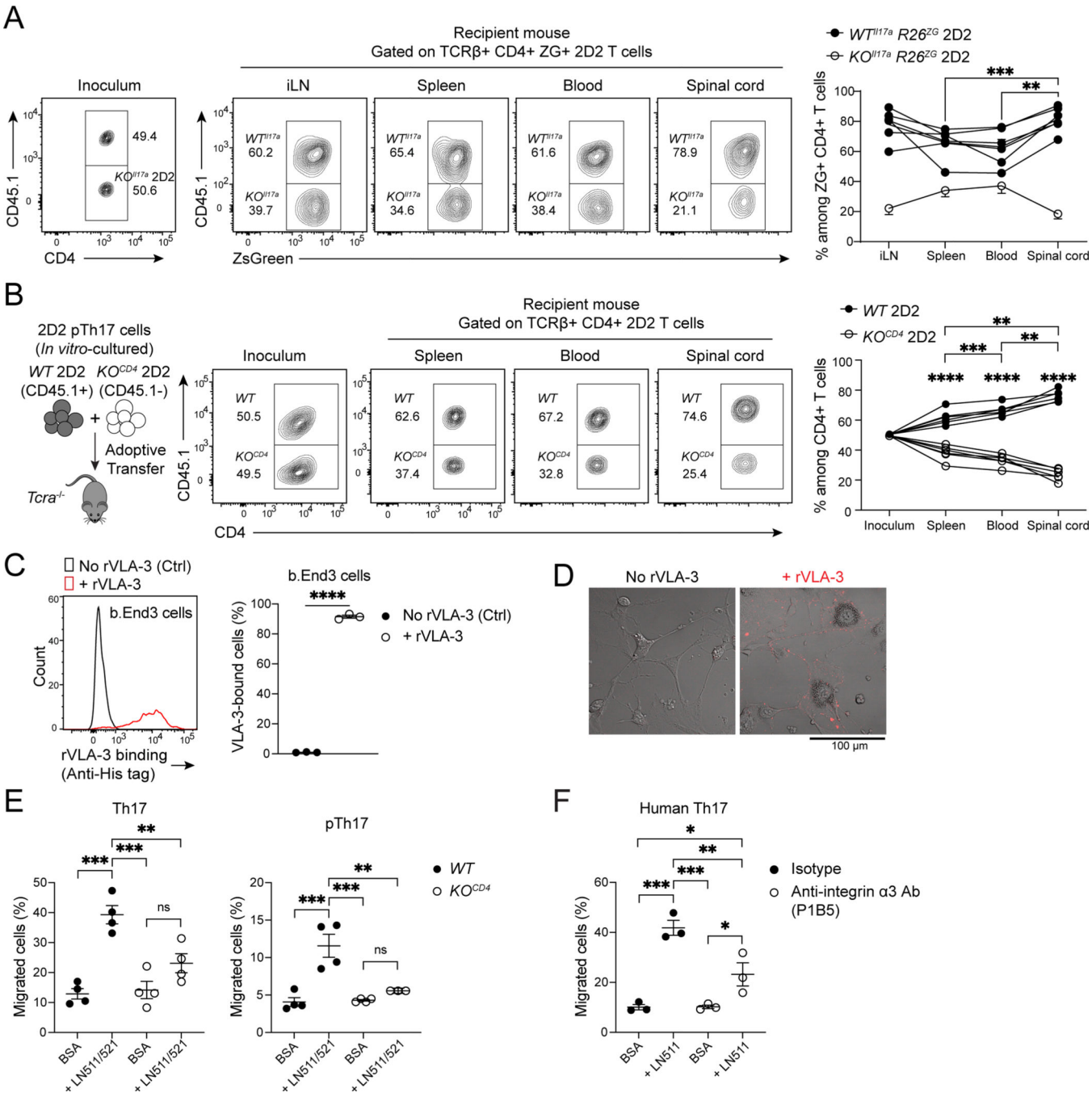

Fig. 8. Integrin α3 promotes the infiltration of Th17 cells into the CNS.

(A) The percentage of WT^{Il17a} $R26^{ZG}$ 2D2 ($CD45.1^{+}$) and KO^{Il17a} $R26^{ZG}$ 2D2 ($CD45.1^{-}$) cells among ZG^{+} $CD4^{+}$ T cells for the transfer experiment performed as in Fig. 6B was analyzed for indicated tissues. $n = 6$ mice, representative of 2 independent experiments. **(B)** The percentage of *WT* and KO^{CD4} $CD4^{+}$ T cells was analyzed for indicated tissues at day 14 post adoptive transfer of *in vitro*-cultured *WT* ($CD45.1^{+}$) or KO^{CD4} ($CD45.1^{-}$) 2D2 pTh17 mixed at a 1:1 ratio (Recipient mice: $Tcra^{-/-}$, $n = 6$, clinical score: 1.5 ± 0.55, representative of 3 independent experiments). **(C)** Flow cytometric analysis of rVLA-3 binding to b.End3

Author Manuscript Author Manuscript Author Manuscript Author Manuscript

cells (pooled from 3 independent experiments). **(D)** Fluorescent live cell images showing rVLA-3 binding to b.End3 cells, representative of 2 independent experiments. Phase contrast is overlaid to highlight cell morphology. **(E)** Summary of transwell migration assay showing the percentage of Th17 or pTh17 cells that migrated to the bottom chamber filled with complete RPMI 1640 media after 6 h. $n = 4$ mice/genotype, pooled from 4 independent experiments. **(F)** Summary of transwell migration assay showing the percentage of hTh17 cells that migrated to bottom chamber filled with complete RPMI 1640 media after 6 h. $n = 3$ donors, pooled from 3 independent experiments. Data acquired from the same recipient mouse are connected by lines (WT^{Il17a} $R26^{ZG}$ 2D2 of **A and B**). Data are summarized as mean ± SEM. Unpaired Student's *t*-test **(B-D)** or paired Student's *t*-test (**A and B**: between different organs). Two-way ANOVA test **(E** and **F)**. *, $p < 0.05$; **, $p < 0.01$; ***, $p < 0.001$; ****, $p < 0.0001$; ns, not significant.